



HAL
open science

Structurally stable but functionally disrupted marine microbial communities under a future climate change scenario: Potential importance for nitrous oxide emissions

Annabelle Dairain, Helena Voet, Anna-Maria Vafeiadou, Nele de Meester, Annelien Rigaux, Carl van Colen, Jan Vanaverbeke, Tom Moens

► To cite this version:

Annabelle Dairain, Helena Voet, Anna-Maria Vafeiadou, Nele de Meester, Annelien Rigaux, et al.. Structurally stable but functionally disrupted marine microbial communities under a future climate change scenario: Potential importance for nitrous oxide emissions. *Science of the Total Environment*, In press, 10.1016/j.scitotenv.2023.167928 . hal-04250779

HAL Id: hal-04250779

<https://hal.science/hal-04250779>

Submitted on 20 Oct 2023

HAL is a multi-disciplinary open access archive for the deposit and dissemination of scientific research documents, whether they are published or not. The documents may come from teaching and research institutions in France or abroad, or from public or private research centers.

L'archive ouverte pluridisciplinaire **HAL**, est destinée au dépôt et à la diffusion de documents scientifiques de niveau recherche, publiés ou non, émanant des établissements d'enseignement et de recherche français ou étrangers, des laboratoires publics ou privés.

1 **Structurally stable but functionally disrupted marine microbial communities**
2 **under a future climate change scenario: potential importance for nitrous oxide**
3 **emissions**

4 **Running title** Marine microbes' sensitivity to global change

5 Annabelle Dairain^{1,3*}, Helena Voet^{1,2}, Anna-Maria Vafeiadou¹, Nele De Meester¹, Annelien Rigaux¹, Carl
6 Van Colen¹, Jan Vanaverbeke^{1,2} and Tom Moens¹

7 ¹ Marine Biology Research Group, Department of Biology, Ghent University, Krijgslaan 281/S8, Ghent
8 9000, Belgium

9
10 ² Royal Belgian Institute of Natural Sciences, Operational Directorate Natural Environment, Marine
11 Ecology and Management, Vautierstraat 29, Brussels 1000, Belgium

12
13 ³ Sorbonne Université, CNRS, Station Biologique de Roscoff, UMR7144, Adaptation et Diversité en Milieu
14 Marin, Place Georges Teissier, CS90074, 29688 Roscoff Cedex, France

15
16 * corresponding author: annabelle.dairain@sorbonne-universite.fr

17

18 **Abstract**

19 The blue mussel *Mytilus edulis* is a widespread and abundant bivalve species along the North Sea with
20 high economic and ecological importance as an engineer species. The shell of mussels is intensively
21 colonized by microbial organisms that can produced significant quantities of nitrous oxide (N₂O), a potent
22 greenhouse gas. To characterize the impacts of climate change on the composition, structure and functioning
23 of microbial biofilms on the shell surface of *M. edulis*, we experimentally exposed them to orthogonal
24 combinations of increased seawater temperature (20 vs. 23 °C) and decreased pH (8.0 vs. 7.7) for six weeks.
25 We used amplicon sequencing of the 16S rRNA gene to characterize the alpha and beta diversity of
26 microbial communities on the mussel shell. The functioning of microbial biofilms was assessed by
27 measuring aerobic respiration and nitrogen emission rates. We did not report any significant impacts of
28 climate change treatments on the diversity of mussel microbiomes nor on the structure of these communities.
29 Lowered pH and increased temperature had antagonistic effects on the functioning of microbial
30 communities with decreased aerobic respiration and N₂O emission rates of microbial biofilms in acidified
31 seawater compared to increased rates in warmer conditions. An overriding impact of acidification over
32 warming was finally observed on N₂O emissions when the two factors were combined. Although
33 acidification and warming in combination significantly reduced N₂O biofilm emissions, the promotion of
34 aquaculture activities in coastal waters where shellfish do not normally occur at high biomass and density
35 could nonetheless result in unwanted emissions of this greenhouse gas in a near future.

36

37 **Key words:** ocean acidification; ocean warming; microbial biofilms; bivalves; nitrogen fluxes, greenhouse
38 gas emission.

39 1. Introduction

40 Since the beginning of the Industrial Revolution, anthropogenic carbon dioxide (CO₂) emissions have
41 constantly increased and contributed to a raise in the global mean sea surface temperature (SST) of 0.68-
42 1.01°C and a decrease of ocean surface pH of 0.1 units (IPCC, 2022). These shifts are expected to continue
43 with a further mean pH decrease of 0.08-0.37 units and a mean temperature increase of 0.86-2.89°C by the
44 end of this century relative to the 1986-2005 period under the shared socio-economic pathway (SSP) 1-2.6
45 and 5-8.5. Changes in seawater pH and temperature have direct physical and chemical consequences such
46 as alteration of gas solubility, enhanced evaporation rates, modified seawater carbonate equilibria or changes
47 in salinity (Bindoff et al., 2019; Hoegh-Guldberg et al., 2014; Pörtner et al., 2014). They also have knock-
48 on impacts on marine biogeochemistry and ecology (Bindoff et al., 2019; Harvey et al., 2013; Pörtner et al.,
49 2014).

50 The nitrogen cycle consists of a series of microbially mediated oxidation-reduction transformations which
51 are sensitive to changes in pH and temperature (Beman et al., 2011; Hicks et al., 2018; Kitidis et al., 2011),
52 hence ocean acidification (OA) and warming (OW) may critically influence the roles of microbes in the
53 nitrogen cycle (Cavicchioli et al., 2019; Currie et al., 2017; Hutchins & Fu, 2017). For instance, projected
54 future seawater *p*CO₂ is expected to lower ammonia oxidation rates of oceanic microbial communities
55 (Beman et al., 2011) while enhancing their nitrogen fixation rate (Hutchins et al., 2007; Lomas et al., 2012).
56 Changes in oceanic pH can indeed affect the availability of substrates for nitrogen transformations such as
57 the NH₃-NH₄⁺ equilibrium (Bange, 2008). Additionally, OA and OW have the potential to (1) directly
58 impact the activity and performance of pelagic (e.g., Endres et al., 2014; Grossart et al., 2006; Hutchins et
59 al., 2007; Lindh et al., 2013; Piontek et al., 2009) and benthic (Braeckman et al., 2014; Laverock et al.,
60 2013; Rastelli et al., 2015) microbiota and (2) drive changes in structure and diversity of microbial
61 communities (Currie et al., 2017; Krause et al., 2012; Vezzulli et al., 2012). Impacts of climate change on
62 the structure and functioning of microbial communities have mainly been studied with a focus on either OA
63 or OW as single stressors. However, their combined effects can differ from their individual ones (Lindh et

64 al., 2013; Minich et al., 2018), and interactive effects of OA and OW on marine microbes, as well as their
65 implications for nitrogen cycling, should therefore be investigated.

66 In addition to being affected by global climate change, the nitrogen cycle can also contribute to radiative
67 forcing in the atmosphere as some microbially-mediated redox conversions produce nitrous oxide (N₂O), a
68 potent greenhouse gas (GHG) (Bange et al., 2010; Devol, 2008). While water bodies and (sub)oxic
69 sediments are broadly recognized as important sources of microbial N₂O production (Voss et al., 2013),
70 there are also other biogenic emissions of N₂O. Microbes in the gut and on the gills of marine invertebrates,
71 for instance, can release N₂O during nitrification and respiratory denitrification processes (Heisterkamp et
72 al., 2016, 2010; Welsh and Castadelli, 2004). These two processes also occur in microbial biofilms on the
73 shells of mollusks (Caffrey et al., 2016; Heisterkamp et al., 2013). This biological matrix is an important
74 site of N₂O emissions with up to 94 % of the total mollusk-associated emissions of the GHG due to microbial
75 assemblages on bivalve shells (Heisterkamp et al., 2013).

76 Along European coasts, an increasing number of offshore wind farms (OWF) are being installed to meet
77 the requirements for green renewable energy (Degraer et al., 2020; Wind Europe, 2021). The submerged
78 foundation of wind turbines constitutes an artificial hard substrate (AHS) that is rapidly and intensely
79 colonized by fouling organisms, of which the blue mussel *M. edulis* is commonly one of the most dominant,
80 both in terms of abundance and biomass (De Mesel et al., 2015; Degraer et al., 2020; Lindeboom et al.,
81 2011). This species is of high economic interest, with a production of ca. 170-200 10³ tons per year in Europe
82 (FAO Fisheries Division, Statistics and Information Branch, 2020). Over the next decade, mussel
83 aquaculture will be promoted within OWF concession areas in the North Sea to optimize the use of the
84 available space (Buck et al., 2008, 2004). Blue mussels can emit N₂O *via* the activity of microbial organisms
85 on their outer shell (Heisterkamp et al., 2013). As a result, human actions promoting availability of
86 substrates (bivalve shells) where N₂O is produced might partly counteract the objective of OWF to limit
87 anthropogenic GHG emissions. It is therefore critical to better understand how changes in the marine
88 environment related to OA and OW would affect the biogenic production of N₂O (Hutchins & Fu, 2017;
89 Voss et al., 2013; Wannicke et al., 2018).

90 Here, we conducted laboratory experiments aiming to (1) characterize microbial communities on shells
91 of the blue mussel *M. edulis* in the North Sea; (2) investigate the effects of OA and OW (separately and in
92 combination) on the composition, α -diversity and structure of biofilm microbial communities; and assess
93 the effect of OA and/or OW on (3) the contribution of shell biofilms to nitrogen compounds'
94 production/consumption and (4) the relative abundance of different nitrogen pathways.

Accepted MS

95 **2. Materials and methods**

96 **2.1. Experimental design**

97 A fully crossed factorial experiment was conducted in July-August 2018 to test the separate and combined
98 influence of seawater temperature increase and pH decrease according to the IPCC “business as usual”
99 scenario representative concentration pathway (RCP) 8.5 (IPCC, 2014) on compositional (i.e., the microbial
100 “species”), structural (i.e., the diversity of the microbial “species”) and functional aspects of microbial
101 communities on the shells of blue mussels, *Mytilus edulis*. The warming and acidification factors
102 encompassed two levels each: ambient summer SST in the Belgian part of the North Sea (BPNS) vs. a
103 temperature increase of 3°C, and ambient pH of the BPNS water in summer vs a pH decrease of 0.3 units.
104 The experiment thus consisted of four treatments: (1) “Control”, i.e. ambient SST and pH, (2)
105 “Acidification”, i.e. ambient SST and a 0.3 units decrease in ambient pH, (3) “Warming”, i.e. a 3°C increase
106 in the SST at ambient pH, and (4) “Climate change”, i.e. a 3°C increase in the SST and a decrease in ambient
107 pH of 0.3 units. The experiment lasted six weeks to assess the relatively long-term effects of the investigated
108 stress factors.

109 **2.2. Experimental setup**

110 **2.2.1. Sampling and acclimation of *Mytilus edulis***

111 Adult blue mussels (mean shell length \pm SE = 45.0 \pm 0.3 mm) were sampled in July 2018 off the coast of
112 Nieuwpoort, Belgium (51°11.024’N, 002°39.883’E), at an aquaculture pilot project site where mussels are
113 farmed using longlines. Mussels were maintained in 80-L barrels filled with oxygenated *in situ* seawater
114 and transported within 4 h to the laboratory. The SST and pH at time of sampling were 19.9°C and 7.9,
115 respectively.

116 Back at the laboratory, approximately 200 mussels were added to each of four mesocosms (one per
117 experimental treatment; length = 100 cm, height = 45 cm, width = 70 cm) filled with unfiltered natural
118 seawater (height of the water column = ca. 30 cm). Mussels were left to acclimatize to mesocosm conditions

119 for 24 h before manipulation began (see 2.2.2). Seawater temperature during the acclimation period was
120 20.0°C, salinity was 32.4 and pH was 7.96. Oxygen pumps were placed in each mesocosm to keep the water
121 fully oxygenated throughout acclimation and incubation (see 2.2.2).

122 **2.2.2. Incubation procedure**

123 A large tank supplied each mesocosm with seawater in a closed circuit of ca. 400 L each. Following
124 acclimation (see 2.2.1), seawater temperature and/or pH was increased in steps of 1°C and decreased in
125 steps of 0.1 unit per day over three days, respectively. The seawater temperature was manipulated in the
126 supply tanks using a heater/cooler (TK-200H, TECO®). A sensor (IKS) in each of the four mesocosms
127 continuously recorded seawater temperature in the circuits. Water pH was manipulated by bubbling
128 seawater with pure CO₂. To this end, an electrode (IKS) was placed in each mesocosm and connected to a
129 modular system (aquaristic computer IKS aquastar) to continuously record water pH. Electrodes were
130 calibrated weekly using buffer solutions (MetrOhm, pH = 4 and pH = 7). The CO₂ bubbling method alters
131 dissolved inorganic carbon at constant total alkalinity and is considered efficient to maintain constant
132 conditions over a long period of time (Riebesell et al., 2011). Approximately one third of the total seawater
133 volume for each treatment was renewed weekly. Mesocosms were kept under a 15h30:8h30 light-dark
134 regime throughout the experiment, mimicking the natural day-night regime at time of sampling (summer
135 2018, see 2.1). Air-bubbling systems were added to the mesocosms to keep the water fully oxygenated
136 during the six weeks of the incubation period. A summary of the physico-chemical water parameters for the
137 four treatments throughout the experiment is available in Supplement S1.

138 Throughout the experiment, mussels were fed twice a week by adding 3 mL of a mix of marine microalgae
139 (Shellfish Diet 1800®, Reed Mariculture) to each mesocosm. Mortality of mussels was checked on a daily
140 basis and dead organisms were removed but not replaced. After six weeks, three mussels were randomly
141 sampled in each mesocosm, placed individually in an incubation chamber (diameter = 10 cm, height = 20
142 cm) and their respiration rates and those of their microbial biofilm were assessed (see 2.2.3).

143 **2.2.3. Aerobic respiration of microbial biofilms**

144 The oxygen consumption rate of microbial biofilms on the shells of three randomly sampled blue mussels
145 per mesocosm was measured using a direct flux approach. To assess the respiration rate of the “pure”
146 biofilms, the shells were opened by cutting the posterior adductor muscle and all soft tissues were removed.
147 Empty mussel shells and their microbiome ($N = 3$ per treatment) were then individually placed in incubation
148 chambers (diameter = 10 cm, height = 20 cm) along with water from their respective mesocosms. Control
149 incubation chambers without empty mussel shell were also set up to. Each incubation chamber was then
150 placed in a water bath in which the temperature corresponded to that in the associated treatment. Chambers
151 were then sealed and an oxygen probe (OXROB10, PyroScience) was introduced in the water column
152 through the lid. A magnetic stirrer homogenized the water column. Incubations lasted for 3 h. The 0% and
153 100% oxygen calibration were performed in a sodium ascorbate solution and in the saturated overlying
154 water of the incubation core, respectively, before the beginning of the incubation. Aerobic respiration rate
155 was calculated as the difference in oxygen concentration in the water column between the beginning and
156 end of the incubation divided by its duration. The latter were corrected for bacterioplankton respiration rates
157 using control incubations.

158 **2.2.4. Influence of microbial communities on nitrogen fluxes**

159 During respiration measurements of biofilms on mussel empty shells (see 2.2.3), we assessed the
160 contribution of microbial biofilms to dissolved ammonium (NH_4^+), nitrate (NO_3^-), nitrite (NO_2^-) and nitrous
161 oxide (N_2O) concentrations in the surrounding water. To this end, we sampled 30 and 25 mL of water at the
162 start and end, respectively, of the three-hour incubation to quantify dissolved N_2O and NH_4^+ , NO_3^- and NO_2^-
163 concentrations, respectively. Water samples for N_2O analysis were fixed with 100 μL of a saturated HgCl_2
164 solution and N_2O concentration in the water was determined by column gas chromatography (8610C Gas
165 Chromatograph, SRI Instruments). A continuous flow analyser (SAN++, Skalar) was used to quantify
166 dissolved concentrations of NH_4^+ , NO_3^- and NO_2^- . Concentrations were corrected for background nitrogen.
167 Nitrogen fluxes (net emission or consumption rates) were calculated as the difference between initial and

168 final concentrations relative to the duration of the incubation. At the end of the incubation, mussel shells
169 were individually placed in plastic bags and frozen at -20°C pending DNA extraction (see 2.3).

170 **2.3. DNA extraction and PCR amplification**

171 Microbial biofilms were scraped from the shell surface of frozen mussels using sterile tweezers and razors.
172 Total DNA was obtained using phenol-chloroform extraction. In detail, scraped biofilms were individually
173 placed in 1.5 mL Eppendorf® tubes with 500 µL of Tris/EDTA (TE buffer, 10mM Tris – 1 mM EDTA),
174 500 µL of phenol (ROTI®Phenol, Roth) and 0.5 g zirconia beads. Extracts were mechanically homogenized
175 (Mixer Mill MM400, Retsch; 1 min 25 sec at 30 Hz, 3 times) and centrifuged for 5 min (11,292 rcf at 4°C).
176 The supernatant of each sample was transferred into a new sterile tube with 500 µL of
177 chloroform:isoamylalcohol (25:24:1 v:v:v). Tubes were shaken by hand and then centrifuged for 5 min
178 (11,292 rcf at 4°C). This step was repeated twice before the supernatant was harvested and transferred into
179 a new tube with 50 µL of sodium acetate (3 M), 1 mL of ethanol (96%) and 2 µL of glycogen (20 mg mL⁻¹).
180 Samples were manually mixed and incubated overnight at -20°C. They were then centrifuged for 30 min
181 (18,213 rcf at 4°C); the supernatant was discarded, 1 mL of ethanol (70%) was added and tubes were
182 centrifuged for 5 min (18,213 rcf at 4°C). The content of the collection tube was discarded and the
183 centrifugation step repeated to ensure there was no remaining ethanol. Pellets were air-dried for 20 min
184 before addition of 100 µL of TE buffer. Finally, tubes were incubated for 20 min at 55°C for a complete
185 dissolution of the DNA pellets. DNA extracts were then stored at -20°C pending PCR amplifications.

186 Bacterial and Archaeal V4 regions of the 16S small-subunit rRNA gene were amplified by PCR using the
187 primer pair 515F–806R (Caporaso et al., 2011). Each sample was amplified in three technical replicates.
188 The PCR was carried out in a total volume of 20 µL comprising 4 µL of PCR reaction buffer (Thermo Fisher
189 Scientific), 0.4 µL of dNTP mix (10 mM each), 0.2 µL of DNA polymerase (Phusion™ Hot Start II High-
190 Fidelity DNA polymerase, Thermo Fisher Scientific; 2 U µL⁻¹), 2 µL of extracted DNA, 11.4 µL of
191 nuclease-free water and 1 µL of each primer (10 µM). Next to the target-specific region, the reverse primers
192 contained an identifier index for each sample and an Illumina adapter (Caporaso et al., 2011). The cycling

193 conditions were: 1 cycle of initial activation at 98°C for 30 s, followed by 35 cycles at 98°C for 10 s, 65°C
194 for 30 s and 72°C for 15 s; then a final step at 72°C for 10 min. PCR products were then analyzed by
195 electrophoresis in a 1% w/v agarose gel stained with ethidium bromide. The technical replicates of amplified
196 PCR products for each sample were pooled before purification using the Agencourt AMPure XP PCR
197 Purification kit (Beckman Coulter). The quantity of DNA for each purified amplicon was measured using a
198 Qubit 3.0 fluorometer (Thermo Fisher Scientific). The samples ($N = 12$ in total) were finally pooled using
199 10 ng of amplicon DNA for each, and the library was sent to Edinburgh Genomics, University of Edinburgh,
200 for Illumina MiSeq sequencing using a 2 x 300-bp paired-end protocol.

201 **2.4. Bioinformatics analyses**

202 Sequencing results were analyzed using QIIME 2 (Bolyen et al., 2019). Forward and reverse primers were
203 first removed from the reads. The DADA2 QIIME 2 plugin (Callahan et al., 2016) was then used to detect
204 and remove low-quality regions of the reads (quality scores < 25) and filter chimeric sequences. An
205 amplicon sequence variant (ASV, Callahan et al., 2017) table was produced, with the number of times each
206 ASV was observed in a sample. Taxonomy was assigned to each of the ASVs using the classify-sklearn
207 qiime feature classifier against the SILVA v132 database (Quast et al., 2012). The classified ASV table was
208 filtered by removing all ASVs with a frequency < 0.1 % of the minimum sample depth (minimum number
209 of reads = 32,170 sequences) as well as non-bacterial or archaeal sequences (i.e., mitochondrial and
210 chloroplast 16S sequences). Rarefaction curves indicated that biofilm microbiomes were sequenced at a
211 depth sufficient to capture the diversity of communities under investigation (Supplement S2). A rooted
212 phylogenetic tree was finally generated using the align-to-tree-mafft-fasttree qiime phylogeny command.

213 QIIME 2 output files were analyzed using R v.3.6.2 (2019-12-12) (R Core Team, 2019). For all analyses,
214 data were rarefied down to 32,170 sequences corresponding to the minimum sample depth. The rarefied
215 number of ASVs per sample was used as a measure of species richness. To evaluate the alpha diversity of
216 mussel-associated bacterial communities within each sample, the Shannon-Wiener and Pielou evenness

217 indices were calculated. We also defined the core microbiomes of mussel biofilm samples by identifying a
218 list of ASVs that were shared by at least 90% of the samples (Shade and Handelsman, 2012).

219 The “phylogenetic investigation of communities by reconstruction of unobserved states” approach was
220 applied to predict the functional potential of the microbial communities on mussel shells from ASV
221 taxonomic affiliations (PICRUSt2; Douglas et al., 2019; Langille et al., 2013). The unrarefied ASV table
222 was used as input. We primarily used PICRUSt2 instead of PICRUSt because it does not require input
223 sequences to be operational taxonomic units (OTUs) (Douglas et al., 2019). From the Kyoto encyclopedia
224 of genes and genomes (KEGG) prediction table, we then identified genes predicted to be involved in the
225 nitrogen cycle. According to the KEGG nitrogen metabolism reference pathway
226 (<https://www.genome.jp/kegg/pathway/map/map00910.html>), the following pathways were identified:
227 assimilatory nitrate reduction (K00360, K00366, K00367, K00372), denitrification (K00368, K15864,
228 K04561, K02305, K00376), dissimilatory nitrate reduction to ammonium (DNRA; K00367, K00372,
229 K00360, K00366, K00362, K00363, K03385, K15876), nitrate reduction (first step of denitrification and
230 DNRA; K00370, K00371, K00374, K02567, K02568), nitrification (K10944, K10945, K10946, K10535)
231 and nitrogen fixation (K02588, K02586, K02591, K00531).

232 **2.5. Statistical analyses**

233 **2.5.1. Microbial community composition and structure**

234 One-way analysis of variance (ANOVA) was used to assess the influence of the experimental treatments
235 (four levels: “Control”, “Acidification”, “Warming” and “Climate change”) on alpha diversity metrics and
236 on the proportion of the total microbiome belonging to the core microbiome. Normality of the data and
237 homogeneity of variances were checked using Shapiro-Wilk and Levene tests, respectively. Data were log-
238 transformed when assumptions were not met. Finally, posthoc Tukey tests were conducted to assess
239 significant differences between entities.

240 Principal coordinate analyses (PCoA) based on generalized UniFrac distances (Chen et al., 2012) were
241 used to visualize the effect of the factor “Treatment” on the structure of microbial communities (i.e., relative

242 abundance of the ASVs) associated with the mussel shells. Permutational multivariate analyses of variance
243 (PERMANOVA) (Anderson, 2001) were run to assess the significance of the separation of groups on the
244 PCoA plot (number of permutations = 999). The PERMDISP procedure was used to test the effects of the
245 experimental treatments on among-replicate variability (i.e. dispersion) (Anderson, 2006). We conducted
246 posthoc pairwise comparison tests to assess significant differences between entities when a significant effect
247 of the “Treatment” factor was reported. All analyses were performed with R (R Core Team, 2019).

248 **2.5.2. Functioning of microbial communities**

249 One-way ANOVA was used to assess the effect of experimental treatment on respiration rates and N₂O,
250 NH₄⁺, NO₃⁻ and NO₂⁻ net production/consumption rates of microbial communities on the shell of blue
251 mussels after six weeks of incubation. Posthoc Tukey tests were conducted to assess significant differences
252 between entities. Normality of the data and homogeneity of variances were checked using Shapiro-Wilk and
253 Levene tests, respectively. PERMANOVA was run to evaluate the effect of experimental treatments on the
254 relative abundance of the different nitrogen pathways All analyses were performed with R (R Core Team,
255 2019).

256 **3. Results**

257 **3.1. Survival of mussels**

258 After six weeks of incubation, mussel mortality in the “Control” mesocosm was < 3 % (97.3% survival;
259 $N = 75$) (Supplement S3). A few mussels died after three weeks in the “Warming” treatment and a cumulated
260 mortality of 10.7% was observed after six weeks. Mussel mortality in “Acidification” and “Climate change”
261 mesocosms was observed as soon as three and one days after initiation of the experiment, respectively, and
262 reached 26 and 33.4%, respectively, after six weeks (Supplement S3).

263 **3.2. Microbial communities: alpha diversity**

264 A total of 615,224 amplicon reads were sequenced with a mean of 51,269 reads per sample (range =
265 32,857–67,837 reads). After filtering and removal of rare ASVs and chimeras, 608,737 reads remained, i.e.,
266 the filtering steps reduced the dataset by ca 1.1 %. A total of 226 to 438 ASVs per sample was identified
267 (Supplement S4).

268 There was no significant effect of the experimental treatments on species richness (Fig. 1A; One-way
269 ANOVA, $F = 0.76$, $p = 0.55$), Shannon-Wiener index (Fig. 1B; One-way ANOVA, $F = 0.11$, $p = 0.95$) and
270 Pielou evenness (Fig. 1C; One-way ANOVA, $F = 0.68$, $p = 0.59$).

271 **3.3. Microbial community structure and taxonomic composition**

272 **3.3.1. Community structure**

273 Permutational multivariate analysis of variance (PERMANOVA) revealed a significant effect of the
274 experimental treatment on the microbial community structure (PERMANOVA, pseudo- $F = 1.68$, p -perm =
275 0.004; Permdisp, pseudo- $F = 2.63$, p -perm = 0.11). There was no clear discrimination of the biofilm
276 communities according to treatment along the first two axis of the PCoA ordination plot (Fig. 2A). In
277 contrast, a distinct separation of “Control” and “Acidification” microbial communities along the third axis
278 of the PCoA ordination plot was observed (Fig. 2B). However, this was not supported by PERMANOVA
279 pairwise tests.

280 3.3.2. Taxonomic composition

281 Microbial communities on the shell of mussels were dominated by Bacteroidia, Alphaproteobacteria,
282 Gammaproteobacteria and Planctomycetacia, irrespectively of the experimental treatment (Fig. 3).
283 Together, these four bacterial classes represented 79.2 ± 11.4 to 90.9 ± 0.6 % of the total microbial
284 community (mean \pm SE) (Table 1). At the order level, Flavobacteriales (Bacteroidia), Rhodobacterales
285 (Alphaproteobacteria), Planctomycetales (Planctomycetacia) and, to a lesser extent, Oceanospirillales
286 (Gammaproteobacteria), Verrucomicrobiales (Verrucomicrobiae), Pirellulales (Planctomycetacia), and
287 Rhizobiales (Alphaproteobacteria) dominated the biofilm assemblages (Fig. 3B, Table 1). As suggested by
288 the PCoA ordination plot (Fig. 2A), the relative abundance of the different bacterial classes and orders were
289 similar between the four experimental treatment (Fig. 3, Table 1).

290 3.3.3. Core microbiome

291 Fifteen ASVs were shared between 90% of the mussel biofilm samples and represented 4.7-20.4% of the
292 total number of reads (mean \pm SE = $12.0 \pm 1.3\%$) (Supplement S5) with no significant differences between
293 treatments (one-way ANOVA, $F_{1,3} = 0.36$, $p = 0.78$). The core ASVs belonged to Bacteroidia
294 (Flavobacteriales: Flavobacteriaceae: *Aquimarina*; $N = 9$ ASVs), Planctomycetacia (Planctomycetales:
295 Rubinisphaeraceae: *Planctomicrobium* and *Fuerstia*; $N = 2$ and 3 ASVs, respectively) and
296 Gammaproteobacteria (Oceanospirillales: Nitrincolaceae: *Neptuniibacter*; $N = 1$ ASV). There was no effect
297 of “Treatment” on the structure of the core microbiome (PERMANOVA, pseudo- $F = 1.068$, p -perm = 0.40;
298 Permdisp, pseudo- $F = 0.86$, p -perm = 0.52).

299 3.4. Functional analyses

300 3.4.1. Biofilm respiration rates

301 Respiration rates of microbial communities on the shell of blue mussels ranged between 1.2 and 8.1 μmol
302 $\text{O}_2 \text{ ind}^{-1} \text{ hour}^{-1}$ (Fig. 4). There was a main effect of the “Treatment” factor (one-way ANOVA, $F_3 = 10.9$ and
303 $p < 0.05$) on respiration rates. Posthoc tests showed that acidification caused a decrease in oxygen

304 consumption of biofilms as compared to the control samples. In contrast, the “Warming” (Tukey HSD, $p =$
305 0.45) and “Climate change” (Tukey HSD, $p = 0.16$) treatments did not significantly affect the biofilm
306 respiration rates as compared to the “Control” (Fig. 4).

307 **3.4.2. Emission and consumption of nitrogen compounds**

308 There was a net production of nitrous oxide N_2O by mussel biofilms that ranged between 0.59 and 10.7
309 $nmol N_2O ind.^{-1} h^{-1}$ after six weeks of incubation (Fig. 5A). Treatments significantly affected net N_2O
310 production rates (one-way ANOVA, $F_3 = 1066.4$, $p < 0.001$). In acidified treatment there was a significant
311 reduction in N_2O production compared to “Control” (Fig. 5A; Tukey posthoc test, $p < 0.05$). In contrast, we
312 noted a 3.0-fold increase in the emission rate of N_2O in “Warming” treatment compared to the “Control”
313 (Fig. 5A; Tukey posthoc test, $p < 0.05$). There was also a net production of ammonium NH_4^+ by the shell
314 biofilms (Fig. 5B), but NH_4^+ net emission rates did not significantly vary between treatments (one-way
315 ANOVA, $F_3 = 1.4$, $p = 0.30$). Finally, there was no significant effect of treatments on NO_3^- (Fig. 5C; one-
316 way ANOVA, $F_3 = 0.44$, $p = 0.73$) and NO_2^- (Fig. 5D; one-way ANOVA, $F_3 = 1.3$, $p = 0.35$) fluxes due to
317 a large inter-individual variability.

318 **3.4.3. Predicted nitrogen cycling functional genes**

319 We identified 15-25 nitrogen metabolism KEGG ortholog (KO) genes in the predicted metagenome of
320 each sample. These genes represented 0.13-0.23 % of the total number of predicted KO genes in mussel
321 biofilm samples (Supplement S6). The nitrogen metabolism KO genes belonged to a diverse range of
322 functional pathways, including assimilatory and dissimilatory nitrate reduction to ammonium (DNRA),
323 denitrification, nitrification and nitrogen fixation (Fig. 6). The most common functional pathways were
324 “denitrification” and “dissimilatory nitrate reduction to ammonium”, irrespective of treatments. Together,
325 they accounted for 70.4 to 76.6% of the predicted nitrogen metabolism pathways (Fig. 6). There was no
326 significant effect of experimental treatments on the relative abundance of different nitrogen pathways
327 (PERMANOVA, pseudo- $F = 1.21$, p -perm = 0.35; Permdisp, pseudo- $F = 2.1$, p -perm = 0.16).

328 **4. Discussion**

329 Microbial biofilms on the shell surface of mollusks are important sites of nitrous oxide N₂O production
330 (Heisterkamp et al., 2013, 2010), a potent greenhouse gas. Shellfish constitute more than 45 % of
331 aquaculture production in Europe (*FAO yearbook. Fishery and Aquaculture Statistics 2017*, 2019) and their
332 production could be promoted through the development of large aquaculture areas in European coastal
333 waters (Buck et al., 2008, 2004). This raises concern because enhanced shellfish farming may lead to
334 unwanted emissions of GHG. At the same time, coastal waters are strongly impacted by global climate
335 change (Bindoff et al., 2019; IPCC, 2022) and the importance for N₂O emissions of microbial biofilms on
336 the shells of aquaculture species can therefore not be accurately understood without taking into account
337 anthropogenic impacts on seawater characteristics. Here we demonstrate that biofilm communities on the
338 shells of blue mussels, *Mytilus edulis*, are compositionally (identity of ASVs) and structurally (relative
339 importance of the different ASVs) robust to future climate change, but also that they were functionally
340 affected by both OA and OW. Notably, ocean warming significantly enhanced the biofilm production of
341 N₂O whereas acidification decreased it.

342 **4.1. Compositional and structural responses of microbial communities to climate change**

343 Ocean acidification (OA) and warming (OW), alone or in combination, did not significantly affect alpha
344 diversity nor composition of microbial communities on the shell surface of blue mussels. Such a low
345 compositional and structural susceptibility of biofilm communities to OA, OW, and climate change (CC) is
346 surprising since several studies have reported that bacterioplankton communities (Lindh et al., 2013; Wang
347 et al., 2021), bacterial consortia on living (Mensch et al., 2020, 2016) and inert surfaces (Ferguson et al.,
348 2021) are sensitive to these stressors, notably OW. The blue mussel inhabits coastal areas and microbes on
349 their shell might thus be able to withstand environmental changes projected for the end of the 21st century.
350 Indeed, biofilms on the shells of blue mussels are naturally exposed to naturally fluctuating pH and
351 temperature in their environment since variability in coastal environments encompasses a range of, among
352 others, daily and seasonal variations expected in the global climate change context (Duarte et al., 2013; Joint

353 et al., 2011; Newbold et al., 2012; Wang et al., 2021). Blue mussels may also have influenced the
354 compositional and structural stability of the microbial communities they host on their shell, explaining the
355 biofilms low susceptibility OA and/or OW. Hosts can produce metabolites that can either inhibit growth of
356 some bacteria (Harder et al., 2003; Persson et al., 2011) or promote microbial settlement (Wahl et al., 1994)
357 and thus modulate the colonization of their surface by microbes. Finally, through its own activity, the mussel
358 biofilm itself might have also provided microbial cells with stable micro-environmental conditions.
359 Microbes synthesize and secrete extracellular polymeric substances that can affect the physical and
360 biogeochemical environment in their proximity (Decho, 1990) and could notably help to buffer changing
361 environmental conditions (de Carvalho, 2018; Decho, 1990).

362 **4.2. Functional changes in microbial communities exposed to climate change**

363 While OA and/or OW did not significantly affect the composition of microbial communities nor in the
364 relative abundance of the different groups of microbes, direct measurements of the activity of bacterial
365 consortia reveal significant and contrasting effects of OA and OW on their functioning. In acidified waters,
366 we noted a 2.2 and a 2.6-fold decrease in the respiration rate and N₂O production rate of microbial biofilms,
367 respectively, as compared to the control. In sharp contrast, there was a 3-fold increase in the N₂O production
368 rate but no significant change in the aerobic respiration rate of microbial organisms in the “Warming”
369 treatment. Opposite effects of OA and OW on the functioning of microbial communities are thus observed,
370 as the pH effects counteract the effects of warming, resulting in similar respiration and N₂O production rates
371 in the “Acidification” and “Climate change” treatments. Nonetheless, it remains unclear how OA, OW and
372 CC affect the relative importance of the diverse N₂O emissions pathways, that is nitrification and
373 denitrification (Heisterkamp et al., 2013). Indeed, the predicting analysis (PICRUST2) did not suggest any
374 significant effect of OA, OW nor CC on the relative contribution of the nitrogen transformation pathways
375 and only assumptions can then be made.

376 **4.2.1. Influence of ocean acidification on microbial communities**

377 In mussel shell biofilms, nitrification and denitrification contribute equally to N₂O production
378 (Heisterkamp et al., 2013). Several studies have reported a significant detrimental effect of OA on

379 nitrification activities of marine microbes which could lead to a concomitant lower production of N₂O
380 (Beman et al., 2011; Kitidis et al., 2011; Wannicke et al., 2018). In contrast, the modulating role of OA on
381 denitrification activities of marine microbes is less clear. Some studies have highlighted that OA could
382 enhance microbes' N₂O production by stimulating the activity of denitrifiers (Su et al., 2021; Wu et al.,
383 2022) whereas others did not reveal any significant mean effect of this stressor (Wannicke et al., 2018). In
384 this study, we did not observe any significant accumulation of NH₄⁺ in the "Acidification" treatment but an
385 increase in the aerobic respiration activity of microbial biofilms. Moreover, the oxygen availability was high
386 (ca. 210 μmol O₂ L⁻¹) in the first 1500 μm above the shell surface of blue mussels in acidified water (Voet
387 et al., 2023). Together, it may suggest a low negative effect of OA on the level of activity of ammonia-
388 oxidising bacteria whereas the activity of anoxic denitrifiers, and concomitant emissions of N₂O, might have
389 been limited. Finally, Voet et al. (2023) have also reported that OA decreases the thickness of marine
390 biofilms on the shell of mussels. Therefore, lower production rate of N₂O may results from a combined
391 negative effect of OA on nitrogen transformation pathways (nitrification and/or denitrification) and
392 microbial abundances.

393 **4.2.2. Influence of ocean warming on microbial communities**

394 Warmer temperatures usually enhance microbial activity through stimulatory effects on biochemical
395 reaction rates (Brown et al., 2004; Gillooly et al., 2001; Pomeroy and Wiebe, 2001), and a similar trend was
396 observed here with a substantial increase in the microbial production of N₂O compared to the "Control"
397 treatment. The processes underlying this pattern are expected to involve higher denitrification rates
398 promoted by more favourable conditions for the activity of denitrifiers, notably lower oxygen availability
399 (Battaglia and Joos, 2018; Codispoti, 2010). Indeed, OW tended to enhance the aerobic respiration rates of
400 microbes which lead to reduced dissolved oxygen concentrations in the close vicinity of the shell surface of
401 mussels (ca. 170-190 μmol O₂ L⁻¹ in the first 500 μm above the shell) (Voet et al., 2023).

402 Although there is still little information about the effects of OW on the nitrogen cycle (but see Voet et al.,
403 2023), such indirect stimulatory effects of OW on N₂O emissions are widely expected (Hutchins and Fu,
404 2017; Voss et al., 2013; Wannicke et al., 2018). In particular, the net production of N₂O during

405 denitrification happens at the interface between suboxic and anoxic waters (Bange et al., 2010; Devol, 2008).
406 Global warming could increase ocean stratification, negatively affect O₂ diffusion and lower subsurface
407 oxygen concentrations, and ultimately promote oxygen minimum zones (Gruber, 2011). In this way, it
408 would thus expand favourable denitrifying conditions for microbial organisms and subsequently N₂O
409 production (Battaglia and Joos, 2018; Codispoti, 2010).

410 **4.2.3. Influence of climate change on microbial communities**

411 In this study, the “Acidification” and “Climate change” treatments had similar restricting impacts on the
412 N₂O production by microbial communities on the shell of blue mussels, whereas OW stimulated the
413 production of this GHG. Therefore, OA has an overriding impact over OW. Nonetheless, it remains unclear
414 whether the magnitudes of the OA and CC effects on the different N₂O production pathways are similar.
415 For instance, we observed a net consumption of NO₂⁻ in some replicates of the “Acidification” treatment
416 and a net production in others, whereas there consistently was a clear net production under “Climate
417 change”. Although the high among-replicate variability led to non-significant test results, these tendencies
418 may suggest a lower denitrification rate of microbes in the “Climate change” treatment as compared to the
419 “Acidification” one. Since nitrous oxide production rates are highly similar in the “Acidification” and
420 “Climate change” treatments, it follows that the relative importance of denitrifiers in N₂O production in the
421 climate change scenario may have been reduced while the activity of ammonia-oxidizing microbes may
422 have gained importance. Although the overall singular effects of OA, or OA and OW in combination, on
423 N₂O production could be the same, the nitrogen pathways involved in the production of the GHG may thus
424 be differently affected in the two contexts. Labelling experiments with stable isotopes remain necessary for
425 an accurate characterisation of the underlying mechanisms involved in the nitrous oxide emission under
426 future climate change conditions (Heisterkamp et al., 2013).

427 **4.3. Implications for the nitrogen cycle at the ecosystem level**

428 Our study suggest that climate change might interfere with nitrogen transformations driven by bacterial
429 biofilms on the shell surface of blue mussels, notably denitrification. However, the net and relative

430 importance of this functional shift at the ecosystem level is uncertain. Knowledge of the roles of microbial
431 associations with macrobiota for nitrogen cycling is still limited (Moulton et al., 2016). A few studies have
432 reported that macrobiota can enhance microbially-mediated N transformations (Diaz and Ward, 1997;
433 Moulton et al., 2016) and that the latter can also be quantitatively important. For instance, ammonium
434 oxidation rates of microbes in association with the Californian mussel *M. californianus* exceeded those of
435 seawater alone by at least two orders of magnitude (Pfister and Altabet, 2019). Here, we observed a 2-fold
436 reduction in the GHG emission in the CC treatment as compared to the control. As such, it could be argued
437 that aquaculture installations in the North Sea would not result in unwanted emissions of GHG under future
438 climate change scenarios. Nevertheless, the promotion of the presence of high densities of bivalves and
439 microbial organisms on their shell through offshore wind farms and/or aquaculture installations in areas that
440 are not naturally colonized by mussels will still result in net unwanted emissions of N₂O irrespective of the
441 climate scenario under consideration.

442 **5. Conclusion**

443 In this study, we used an experimental *ex situ* approach to assess the effects of climate change (ocean
444 acidification OA and warming OW, in isolation and in combination) on the composition, diversity and
445 structure of microbial communities associated with the shell of the blue mussel *Mytilus edulis*. We also
446 evaluated the effects of climate change on mussel shell biofilm-associated nitrogen transformations.
447 Predicted changes in seawater pH and/or temperature had negligible effects on the composition, diversity,
448 and structure of microbial biofilms on the outer shell surface of blue mussels. By contrast, substantial
449 functional shifts occurred with respect to the influence of the microorganisms on the nitrogen cycle. In
450 particular, OW increased the nitrous oxide production rate of bacteria on mussel shells, whereas ocean
451 acidification, in isolation and in combination with ocean warming, reduced it. Nonetheless, we cannot
452 conclude about a positive or a negative effect of climate change on net N₂O emissions. Indeed, the artificial
453 expansion of substrates where N₂O is produced through aquaculture could still result in net emissions of the
454 GHG. At the ecosystem level, the importance of these emissions for large-scale processes remains uncertain,

455 but considering that the marine nitrogen cycle is tightly coupled to other major cycles, complementary
456 studies appear critical to better understand interactive effects between marine biogeochemical cycles under
457 future climate change (Battaglia and Joos, 2018).

458

Accepted MS

459 **Compliance with ethical standards**

460 All applicable international, national and/or institutional guidelines for the care and use of animals were
461 followed.

462 **Declarations of interest**

463 The authors declare that they have no known competing financial interests or personal relationships that
464 could have appeared to influence the work reported in this paper.

465 **Funding**

466 The research leading to results presented in this publication was funded through BELSPO BRAIN-be project
467 BR/175/A1/PERSUADE, extra funding obtained from Ghent University's Special Research Fund (BOF)
468 through GOA project 01G02617 and carried out with infrastructure funded by EMBRC Belgium - FWO
469 international research infrastructure I001621N. This work was supported by logistic support from the vessel
470 Stream (Brevisco) and the ILVO aquaculture pilot project Value@Sea (with partners Belwind, Brevisco,
471 Sioen Industries, Colruyt Group, C-Power, DEME, RBINS – OD Nature, Lobster Fish and Ghent
472 University).

473 **Acknowledgements**

474 The authors are grateful to H el ene Moussard, Laure Van den Bulcke, Ellen Vlaminc k, Stefan Van Damme,
475 Ee Zin Ong, Hannelore Theetaert, Bart Beuselinck and Bruno Vlaminc k for their practical and analytical
476 support that was indispensable in the realization of this study. The authors are also grateful to Alberto Borges
477 for his significant help with N₂O analyses.

478 **References**

- 479 Anderson, M.J., 2006. Distance-based tests for homogeneity of multivariate dispersions.
480 *Biometrics* 62, 245–253. <https://doi.org/10.1111/j.1541-0420.2005.00440.x>
- 481 Anderson, M.J., 2001. A new method for non-parametric multivariate analysis of variance.
482 *Austral Ecology* 26, 32–46. <https://doi.org/10.1111/j.1442-9993.2001.01070.pp.x>
- 483 Bange, H.W., 2008. Gaseous nitrogen compounds (NO, N₂O, N₂, NH₃) in the ocean, in:
484 Capone, D.G., Bronk, D.A., Mulholland, M.R., Carpenter, E.J. (Eds.), *Nitrogen in the*
485 *Marine Environment (Second Edition)*. Academic Press, San Diego, pp. 51–94.
486 <https://doi.org/10.1016/B978-0-12-372522-6.00002-5>
- 487 Bange, H.W., Freing, A., Kock, A., Löscher, C.R., 2010. Marine pathways to nitrous oxide, in:
488 *Nitrous Oxide and Climate Change*. London, pp. 26–62.
- 489 Battaglia, G., Joos, F., 2018. Marine N₂O emissions from nitrification and denitrification
490 constrained by modern observations and projected in multimillennial global warming
491 simulations. *Global Biogeochemical Cycles* 32, 92–121.
492 <https://doi.org/10.1002/2017GB005671>
- 493 Beman, J.M., Chow, C.-E., King, A.L., Feng, Y., Fuhrman, J.A., Andersson, A., Bates, N.R.,
494 Popp, B.N., Hutchins, D.A., 2011. Global declines in oceanic nitrification rates as a
495 consequence of ocean acidification. *PNAS* 108, 208–213.
496 <https://doi.org/10.1073/pnas.1011053108>
- 497 Bindoff, N.L., Cheung, W.W.L., Kairo, J.G., Aristegui, J., Guinder, V.A., Hallberg, R., Hilmi,
498 N., Jiao, N., Karim, M.S., Levin, L., O’Donoghue, S., Purca Cuicapusa, S.R., Rinkevich,
499 B., Suga, T., Tagliabue, A., Williamson, P., 2019. IPCC 2019: Changing ocean, marine
500 ecosystems and dependent communities, in: *IPCC Special Report in the Ocean and*
501 *Cryosphere in a Changing Climate*. Cambridge University Press, Cambridge, United
502 Kingdom and New York, NY, USA, pp. 447–587.
- 503 Bolyen, E., Rideout, J.R., Dillon, M.R., Bokulich, N.A., Abnet, C.C., Al-Ghalith, G.A.,
504 Alexander, H., Alm, E.J., Arumugam, M., Asnicar, F., Bai, Y., Bisanz, J.E., Bittinger, K.,
505 Brejnrod, A., Brislawn, C.J., Brown, C.T., Callahan, B.J., Caraballo-Rodríguez, A.M.,
506 Chase, J., Cope, E.K., Da Silva, R., Diener, C., Dorrestein, P.C., Douglas, G.M., Durall,
507 D.M., Duvallet, C., Edwardson, C.F., Ernst, M., Estaki, M., Fouquier, J., Gauglitz, J.M.,
508 Gibbons, S.M., Gibson, D.L., Gonzalez, A., Gorlick, K., Guo, J., Hillmann, B., Holmes,
509 S., Holste, H., Huttenhower, C., Huttley, G.A., Janssen, S., Jarmusch, A.K., Jiang, L.,
510 Kaehler, B.D., Kang, K.B., Keefe, C.R., Keim, P., Kelley, S.T., Knights, D., Koester, I.,
511 Kosciolk, T., Kreps, J., Langille, M.G.I., Lee, J., Ley, R., Liu, Y.-X., Loftfield, E.,
512 Lozupone, C., Maher, M., Marotz, C., Martin, B.D., McDonald, D., McIver, L.J., Melnik,
513 A.V., Metcalf, J.L., Morgan, S.C., Morton, J.T., Naimey, A.T., Navas-Molina, J.A.,
514 Nothias, L.F., Orchanian, S.B., Pearson, T., Peoples, S.L., Petras, D., Preuss, M.L.,
515 Priesse, E., Rasmussen, L.B., Rivers, A., Robeson, M.S., Rosenthal, P., Segata, N.,
516 Shaffer, M., Shiffer, A., Sinha, R., Song, S.J., Spear, J.R., Swafford, A.D., Thompson,
517 L.R., Torres, P.J., Trinh, P., Tripathi, A., Turnbaugh, P.J., Ul-Hasan, S., van der Hooft,
518 J.J.J., Vargas, F., Vázquez-Baeza, Y., Vogtmann, E., von Hippel, M., Walters, W., Wan,
519 Y., Wang, M., Warren, J., Weber, K.C., Williamson, C.H.D., Willis, A.D., Xu, Z.Z.,
520 Zaneveld, J.R., Zhang, Y., Zhu, Q., Knight, R., Caporaso, J.G., 2019. Reproducible,
521 interactive, scalable and extensible microbiome data science using QIIME 2. *Nat*
522 *Biotechnol* 37, 852–857. <https://doi.org/10.1038/s41587-019-0209-9>

- 523 Braeckman, U., Colen, C.V., Guilini, K., Gansbeke, D.V., Soetaert, K., Vincx, M., Vanaverbeke,
524 J., 2014. Empirical evidence reveals seasonally dependent reduction in nitrification in
525 coastal sediments subjected to near future ocean acidification. *PLOS ONE* 9, e108153.
526 <https://doi.org/10.1371/journal.pone.0108153>
- 527 Brown, J.H., Gillooly, J.F., Allen, A.P., Savage, V.M., West, G.B., 2004. Toward a metabolic
528 theory of ecology. *Ecology* 85, 1771–1789. <https://doi.org/10.1890/03-9000>
- 529 Buck, B.H., Krause, G., Michler-Cieluch, T., Brenner, M., Buchholz, C.M., Busch, J.A., Fisch,
530 R., Geisen, M., Zielinski, O., 2008. Meeting the quest for spatial efficiency: progress and
531 prospects of extensive aquaculture within offshore wind farms. *Helgol Mar Res* 62, 269–
532 281. <https://doi.org/10.1007/s10152-008-0115-x>
- 533 Buck, B.H., Krause, G., Rosenthal, H., 2004. Extensive open ocean aquaculture development
534 within wind farms in Germany: the prospect of offshore co-management and legal
535 constraints. *Ocean & Coastal Management* 47, 95–122.
536 <https://doi.org/10.1016/j.ocecoaman.2004.04.002>
- 537 Caffrey, J.M., Hollibaugh, J.T., Mortazavi, B., 2016. Living oysters and their shells as sites of
538 nitrification and denitrification. *Marine Pollution Bulletin* 112, 86–90.
539 <https://doi.org/10.1016/j.marpolbul.2016.08.038>
- 540 Callahan, B.J., McMurdie, P.J., Holmes, S.P., 2017. Exact sequence variants should replace
541 operational taxonomic units in marker-gene data analysis. *ISME J* 11, 2639–2643.
542 <https://doi.org/10.1038/ismej.2017.119>
- 543 Callahan, B.J., McMurdie, P.J., Rosen, M.J., Han, A.W., Johnson, A.J.A., Holmes, S.P., 2016.
544 DADA2: High-resolution sample inference from Illumina amplicon data. *Nat Methods*
545 13, 581–583. <https://doi.org/10.1038/nmeth.3869>
- 546 Caporaso, J.G., Lauber, C.L., Walters, W.A., Berg-Lyons, D., Lozupone, C.A., Turnbaugh, P.J.,
547 Fierer, N., Knight, R., 2011. Global patterns of 16S rRNA diversity at a depth of millions
548 of sequences per sample. *Proceedings of the National Academy of Sciences* 108, 4516–
549 4522. <https://doi.org/10.1073/pnas.1000080107>
- 550 Cavicchioli, R., Ripple, W.J., Timmis, K.N., Azam, F., Bakken, L.R., Baylis, M., Behrenfeld,
551 M.J., Boetius, A., Boyd, P.W., Classen, A.T., Crowther, T.W., Danovaro, R., Foreman,
552 C.M., Huisman, J., Hutchins, D.A., Jansson, J.K., Karl, D.M., Koskella, B., Mark Welch,
553 D.B., Martiny, J.B.H., Moran, M.A., Orphan, V.J., Reay, D.S., Remais, J.V., Rich, V.I.,
554 Singh, B.K., Stein, L.Y., Stewart, F.J., Sullivan, M.B., van Oppen, M.J.H., Weaver, S.C.,
555 Webb, E.A., Webster, N.S., 2019. Scientists’ warning to humanity: microorganisms and
556 climate change. *Nat Rev Microbiol* 17, 569–586. <https://doi.org/10.1038/s41579-019-0222-5>
- 558 Chen, J., Bittinger, K., Charlson, E.S., Hoffmann, C., Lewis, J., Wu, G.D., Collman, R.G.,
559 Bushman, F.D., Li, H., 2012. Associating microbiome composition with environmental
560 covariates using generalized UniFrac distances. *Bioinformatics* 28, 2106–2113.
561 <https://doi.org/10.1093/bioinformatics/bts342>
- 562 Codispoti, L.A., 2010. Interesting times for marine N₂O. *Science* 327, 1339–1340.
563 <https://doi.org/10.1126/science.1184945>
- 564 Currie, A.R., Tait, K., Parry, H., de Francisco-Mora, B., Hicks, N., Osborn, A.M., Widdicombe,
565 S., Stahl, H., 2017. Marine microbial gene abundance and community composition in
566 response to ocean acidification and elevated temperature in two contrasting coastal marine
567 sediments. *Front. Microbiol.* 8, 1599. <https://doi.org/10.3389/fmicb.2017.01599>
- 568 de Carvalho, C.C.C.R., 2018. Marine biofilms: a successful microbial strategy with economic
569 implications. *Front. Mar. Sci.* 5, 126. <https://doi.org/10.3389/fmars.2018.00126>

- 570 De Mesel, I., Kerckhof, F., Norro, A., Rumes, B., Degraer, S., 2015. Succession and seasonal
571 dynamics of the epifauna community on offshore wind farm foundations and their role as
572 stepping stones for non-indigenous species. *Hydrobiologia* 756, 37–50.
573 <https://doi.org/10.1007/s10750-014-2157-1>
- 574 Decho, A.W., 1990. Microbial exopolymer secretions in ocean environments: their role(s) in food
575 webs and marine processes, in: *Oceanography and Marine Biology - An Annual Review*.
576 Margaret Barnes, Aberdeen, pp. 73–153.
- 577 Degraer, S., Carey, D., Coolen, J., Hutchison, Z., Kerckhof, F., Rumes, B., Vanaverbeke, J.,
578 2020. Offshore wind farm artificial reefs affect ecosystem structure and functioning: a
579 synthesis. *Oceanog* 33, 48–57. <https://doi.org/10.5670/oceanog.2020.405>
- 580 Devol, A.H., 2008. Denitrification Including Anammox, in: *Nitrogen in the Marine Environment*.
581 Elsevier, Amsterdam, pp. 263–301. <https://doi.org/10.1016/B978-0-12-372522-6.00006-2>
- 582 Diaz, M., Ward, B., 1997. Sponge-mediated nitrification in tropical benthic communities. *Mar.*
583 *Ecol. Prog. Ser.* 156, 97–107. <https://doi.org/10.3354/meps156097>
- 584 Douglas, G.M., Maffei, V.J., Zaneveld, J., Yurgel, S.N., Brown, J.R., Taylor, C.M., Huttenhower,
585 C., Langille, M.G.I., 2019. PICRUSt2: An improved and customizable approach for
586 metagenome inference (preprint). *Bioinformatics*. <https://doi.org/10.1101/672295>
- 587 Duarte, C.M., Hendriks, I.E., Moore, T.S., Olsen, Y.S., Steckbauer, A., Ramajo, L., Carstensen,
588 J., Trotter, J.A., McCulloch, M., 2013. Is ocean acidification an open-ocean syndrome?
589 Understanding anthropogenic impacts on seawater pH. *Estuaries and Coasts* 36, 221–236.
590 <https://doi.org/10.1007/s12237-013-9594-3>
- 591 Endres, S., Galgani, L., Riebesell, U., Schulz, K.-G., Engel, A., 2014. Stimulated bacterial
592 growth under elevated pCO₂: results from an off-shore mesocosm study. *PLoS ONE* 9,
593 e99228. <https://doi.org/10.1371/journal.pone.0099228>
- 594 FAO Fisheries Division, Statistics and Information Branch, 2020. FishStatJ: Universal software
595 for fishery statistical time series.
- 596 FAO yearbook. Fishery and Aquaculture Statistics 2017, 2019. . FAO, Rome.
- 597 Ferguson, R.M.W., O’Gorman, E.J., McElroy, D.J., McKew, B.A., Coleman, R.A., Emmerson,
598 M.C., Dumbrell, A.J., 2021. The ecological impacts of multiple environmental stressors
599 on coastal biofilm bacteria. *Global Change Biology* 27, 3166–3178.
600 <https://doi.org/10.1111/gcb.15626>
- 601 Gillooly, J.F., Brown, J.H., West, G.B., Savage, V.M., Charnov, E.L., 2001. Effects of size and
602 temperature on metabolic rate. *Science* 293, 2248–2251.
603 <https://doi.org/10.1126/science.1061967>
- 604 Grossart, H.-P., Allgaier, M., Passow, U., Riebesell, U., 2006. Testing the effect of CO₂
605 concentration on the dynamics of marine heterotrophic bacterioplankton. *Limnology and*
606 *Oceanography* 51, 1–11. <https://doi.org/10.4319/lo.2006.51.1.0001>
- 607 Gruber, N., 2011. Warming up, turning sour, losing breath: ocean biogeochemistry under global
608 change. *Philosophical Transactions of the Royal Society A: Mathematical, Physical and*
609 *Engineering Sciences* 1980–1996. <https://doi.org/10.1098/rsta.2011.0003>
- 610 Harder, T., Lau, S.C.K., Dobretsov, S., Fang, T.K., Qian, P.-Y., 2003. A distinctive epibiotic
611 bacterial community on the soft coral *Dendronephthya* sp. and antibacterial activity of
612 coral tissue extracts suggest a chemical mechanism against bacterial epibiosis. *FEMS*
613 *Microbiology Ecology* 43, 337–347. <https://doi.org/10.1111/j.1574-6941.2003.tb01074.x>
- 614 Harvey, B.P., Gwynn-Jones, D., Moore, P.J., 2013. Meta-analysis reveals complex marine
615 biological responses to the interactive effects of ocean acidification and warming. *Ecol*
616 *Evol* 3, 1016–1030. <https://doi.org/10.1002/ece3.516>

617 Heisterkamp, I.M., Schramm, A., de Beer, D., Stief, P., 2016. Direct nitrous oxide emission from
618 the aquacultured Pacific white shrimp (*Litopenaeus vannamei*). Appl. Environ. Microbiol.
619 82, 4028–4034. <https://doi.org/10.1128/AEM.00396-16>

620 Heisterkamp, I.M., Schramm, A., de Beer, D., Stief, P., 2010. Nitrous oxide production
621 associated with coastal marine invertebrates. Mar. Ecol. Prog. Ser. 415, 1–9.
622 <https://doi.org/10.3354/meps08727>

623 Heisterkamp, I.M., Schramm, A., Larsen, L.H., Svenningsen, N.B., Lavik, G., de Beer, D., Stief,
624 P., 2013. Shell biofilm-associated nitrous oxide production in marine molluscs: processes,
625 precursors and relative importance. Environmental microbiology 15, 1943–1955.
626 <https://doi.org/10.1111/j.1462-2920.2012.02823.x>

627 Hicks, N., Liu, X., Gregory, R., Kenny, J., Lucaci, A., Lenzi, L., Paterson, D.M., Duncan, K.R.,
628 2018. Temperature driven changes in benthic bacterial diversity influences
629 biogeochemical cycling in coastal sediments. Front. Microbiol. 9, 1730.
630 <https://doi.org/10.3389/fmicb.2018.01730>

631 Hoegh-Guldberg, O., Cai, R., Poloczanska, E.S., Brewer, P.G., Sundby, S., Hilmi, K., Fabry,
632 V.J., Jung, S., 2014. The Ocean, in: Climate Change 2014: Impacts, Adaptation, and
633 Vulnerability. Part B: Regional Aspects. Contribution of Working Group II to the Fifth
634 Assessment Report of the Intergovernmental Panel on Climate Change. Cambridge,
635 United Kingdom and New York, NY, USA, pp. 1655–1731.

636 Hutchins, D.A., Fu, F., 2017. Microorganisms and ocean global change. Nature Microbiology 2,
637 1–11. <https://doi.org/10.1038/nmicrobiol.2017.58>

638 Hutchins, D.A., Fu, F.-X., Zhang, Y., Warner, M.E., Feng, Y., Portune, K., Bernhardt, P.W.,
639 Mulholland, M.R., 2007. CO₂ control of *Trichodesmium* N₂ fixation, photosynthesis,
640 growth rates, and elemental ratios: Implications for past, present, and future ocean
641 biogeochemistry. Limnology and Oceanography 52, 1293–1304.
642 <https://doi.org/10.4319/lo.2007.52.4.1293>

643 IPCC, 2022. Climate Change 2022: Impacts, Adaptation and Vulnerability. Working Group II
644 contribution to the Sixth Assessment Report of the Intergovernmental Panel on Climate
645 Change. Cambridge University Press.

646 IPCC, 2014. Climate Change 2014: Synthesis Report. Contribution of Working Groups I, II and
647 III to the Fifth Assessment Report of the Intergovernmental Panel on Climate Change.
648 Core Writing Team, R.K. Pachauri and L.A. Meyer (eds.), Geneva, Switzerland.

649 Joint, I., Doney, S.C., Karl, D.M., 2011. Will ocean acidification affect marine microbes? The
650 ISME Journal 5, 1–7. <https://doi.org/10.1038/ismej.2010.79>

651 Kitidis, V., Laverock, B., McNeill, L.C., Beesley, A., Cummings, D., Tait, K., Osborn, M.A.,
652 Widdicombe, S., 2011. Impact of ocean acidification on benthic and water column
653 ammonia oxidation. Geophysical Research Letters 38.
654 <https://doi.org/10.1029/2011GL049095>

655 Krause, E., Wichels, A., Giménez, L., Lunau, M., Schilhabel, M.B., Gerds, G., 2012. Small
656 changes in pH have direct effects on marine bacterial community composition: a
657 microcosm approach. PLoS ONE 7, e47035.
658 <https://doi.org/10.1371/journal.pone.0047035>

659 Langille, M.G.I., Zaneveld, J., Caporaso, J.G., McDonald, D., Knights, D., Reyes, J.A.,
660 Clemente, J.C., Burkepille, D.E., Thurber, R.L.V., Knight, R., Beiko, R.G., Huttenhower,
661 C., 2013. Predictive functional profiling of microbial communities using 16S rRNA
662 marker gene sequences. Nat Biotechnol 31, 814–821. <https://doi.org/10.1038/nbt.2676>

- 663 Laverock, B., Kitidis, V., Tait, K., Gilbert, J.A., Osborn, A.M., Widdicombe, S., 2013.
664 Bioturbation determines the response of benthic ammonia-oxidizing microorganisms to
665 ocean acidification. *Phil. Trans. R. Soc. B* 368, 20120441.
666 <https://doi.org/10.1098/rstb.2012.0441>
- 667 Lindeboom, H.J., Kouwenhoven, H.J., Bergman, M.J.N., Bouma, S., Brasseur, S., Daan, R., Fijn,
668 R.C., Haan, D. de, Dirksen, S., Hal, R. van, Lambers, R.H.R., Hofstede, R. ter,
669 Krijgsveld, K.L., Leopold, M., Scheidat, M., 2011. Short-term ecological effects of an
670 offshore wind farm in the Dutch coastal zone. *Environ. Res. Lett.* 6, 035101. <https://doi.org/10.1088/1748-9326/6/3/035101>
- 671 Lindh, M.V., Riemann, L., Baltar, F., Romero-Oliva, C., Salomon, P.S., Granéli, E., Pinhassi, J.,
672 2013. Consequences of increased temperature and acidification on bacterioplankton
673 community composition during a mesocosm spring bloom in the Baltic Sea.
674 *Environmental Microbiology Reports* 5, 252–262. <https://doi.org/10.1111/1758-2229.12009>
- 675 Lomas, M.W., Hopkinson, B.M., Ryan, J.L.L.D.E., Shi, D.L., Xu, Y., Morel, F.M.M., 2012.
676 Effect of ocean acidification on cyanobacteria in the subtropical North Atlantic. *Aquatic
677 Microbial Ecology* 66, 211–222. <https://doi.org/10.3354/ame01576>
- 678 Mensch, B., Neulinger, S.C., Graiff, A., Pansch, A., Künzel, S., Fischer, M.A., Schmitz, R.A.,
679 2016. Restructuring of epibacterial communities on *Fucus vesiculosus forma mytili* in
680 response to elevated pCO₂ and increased temperature levels. *Front. Microbiol.* 7.
681 <https://doi.org/10.3389/fmicb.2016.00434>
- 682 Mensch, B., Neulinger, S.C., Künzel, S., Wahl, M., Schmitz, R.A., 2020. Warming, but not
683 acidification, restructures epibacterial communities of the Baltic macroalga *Fucus
684 vesiculosus* with seasonal variability. *Front. Microbiol.* 11, 1471.
685 <https://doi.org/10.3389/fmicb.2020.01471>
- 686 Minich, J.J., Morris, M.M., Brown, M., Doane, M., Edwards, M.S., Michael, T.P., Dinsdale,
687 E.A., 2018. Elevated temperature drives kelp microbiome dysbiosis, while elevated
688 carbon dioxide induces water microbiome disruption. *PLOS ONE* 13, e0192772.
689 <https://doi.org/10.1371/journal.pone.0192772>
- 690 Moulton, O.M., Altabet, M.A., Beman, J.M., Deegan, L.A., Lloret, J., Lyons, M.K., Nelson, J.A.,
691 Pfister, C.A., 2016. Microbial associations with macrobiota in coastal ecosystems:
692 patterns and implications for nitrogen cycling. *Front Ecol Environ* 14, 200–208.
693 <https://doi.org/10.1002/fee.1262>
- 694 Newbold, L.K., Oliver, A.E., Booth, T., Tiwari, B., DeSantis, T., Maguire, M., Andersen, G., van
695 der Gast, C.J., Whiteley, A.S., 2012. The response of marine picoplankton to ocean
696 acidification. *Environmental Microbiology* 14, 2293–2307.
697 <https://doi.org/10.1111/j.1462-2920.2012.02762.x>
- 698 Persson, F., Svensson, R., Nylund, G.M., Fredriksson, N.J., Pavia, H., Hermansson, M., 2011.
699 Ecological role of a seaweed secondary metabolite for a colonizing bacterial community.
700 *Biofouling* 27, 579–588. <https://doi.org/10.1080/08927014.2011.589001>
- 701 Pfister, C.A., Altabet, M.A., 2019. Enhanced microbial nitrogen transformations in association
702 with macrobiota from the rocky intertidal. *Biogeosciences* 16, 193–206.
703 <https://doi.org/10.5194/bg-16-193-2019>
- 704 Piontek, J., Händel, N., Langer, G., Wohlers, J., Riebesell, U., Engel, A., 2009. Effects of rising
705 temperature on the formation and microbial degradation of marine diatom aggregates.
706 *Aquatic Microbial Ecology* 54, 305–318. <https://doi.org/10.3354/ame01273>
- 707
708

709 Pomeroy, L., Wiebe, W., 2001. Temperature and substrates as interactive limiting factors for
710 marine heterotrophic bacteria. *Aquat. Microb. Ecol.* 23, 187–204.
711 <https://doi.org/10.3354/ame023187>

712 Pörtner, H.O., Karl, D.M., Boyd, P.W., Cheung, W.W.L., Lluch, S.E., Nojiri, Y., Schmidt, D.N.,
713 Zaviyalov, P.O., 2014. Ocean systems, in: *Climate Change 2014: Impacts, Adaptation, and*
714 *Vulnerability. Part A: Global and Sectoral Aspects. Contribution of Working Group II to*
715 *the Fifth Assessment Report of the Intergovernmental Panel on Climate Change.*
716 Cambridge, United Kingdom and New York, NY, USA, pp. 411–484.

717 Quast, C., Pruesse, E., Yilmaz, P., Gerken, J., Schweer, T., Yarza, P., Peplies, J., Glöckner, F.O.,
718 2012. The SILVA ribosomal RNA gene database project: improved data processing and
719 web-based tools. *Nucleic Acids Research* 41, D590–D596.
720 <https://doi.org/10.1093/nar/gks1219>

721 R Core Team, 2019. R: a language and environment for statistical computing.

722 Rastelli, E., Corinaldesi, C., Dell’Anno, A., Amaro, T., Queiros, A.M., Widdicombe, S.,
723 Danovaro, R., 2015. Impact of CO₂ leakage from sub-seabed carbon dioxide capture and
724 storage (CCS) reservoirs on benthic virus–prokaryote interactions and functions. *Front.*
725 *Microbiol.* 0. <https://doi.org/10.3389/fmicb.2015.00935>

726 Riebesell, U., Fabry, V.J., Hansson, L., Gattuso, J.-P., 2011. Guide to best practices for ocean
727 acidification research and data reporting. Office for Official Publications of the European
728 Communities, Brussels.

729 Shade, A., Handelsman, J., 2012. Beyond the Venn diagram: the hunt for a core microbiome.
730 *Environmental Microbiology* 14, 4–12. <https://doi.org/10.1111/j.1462-2920.2011.02585.x>

731 Su, X., Wen, T., Wang, Y., Xu, J., Cui, L., Zhang, J., Xue, X., Ding, K., Tang, Y., Zhu, Y., 2021.
732 Stimulation of N₂ O emission via bacterial denitrification driven by acidification in
733 estuarine sediments. *Global Change Biology* 27, 5564–5579.
734 <https://doi.org/10.1111/gcb.15863>

735 Vezzulli, L., Brettar, I., Pezzati, E., Reid, P.C., Colwell, R.R., Höfle, M.G., Pruzzo, C., 2012.
736 Long-term effects of ocean warming on the prokaryotic community: evidence from the
737 vibrios. *ISME J* 6, 21–30. <https://doi.org/10.1038/ismej.2011.89>

738 Voet, H., Soetaert, K., Moens, T., Bodé, S., Boeckx, P., Van Colen, C., Vanaverbeke, J., 2023.
739 N₂O production by mussels: Quantifying rates and pathways in current and future climate
740 settings. *Front. Mar. Sci.* 10, 1101469. <https://doi.org/10.3389/fmars.2023.1101469>

741 Voss, M., Bange, H.W., Dippner, J.W., Middelburg, J.J., Montoya, J.P., Ward, B., 2013. The
742 marine nitrogen cycle: recent discoveries, uncertainties and the potential relevance of
743 climate change. *Philosophical Transactions of the Royal Society B: Biological Sciences*
744 368, 20130121. <https://doi.org/10.1098/rstb.2013.0121>

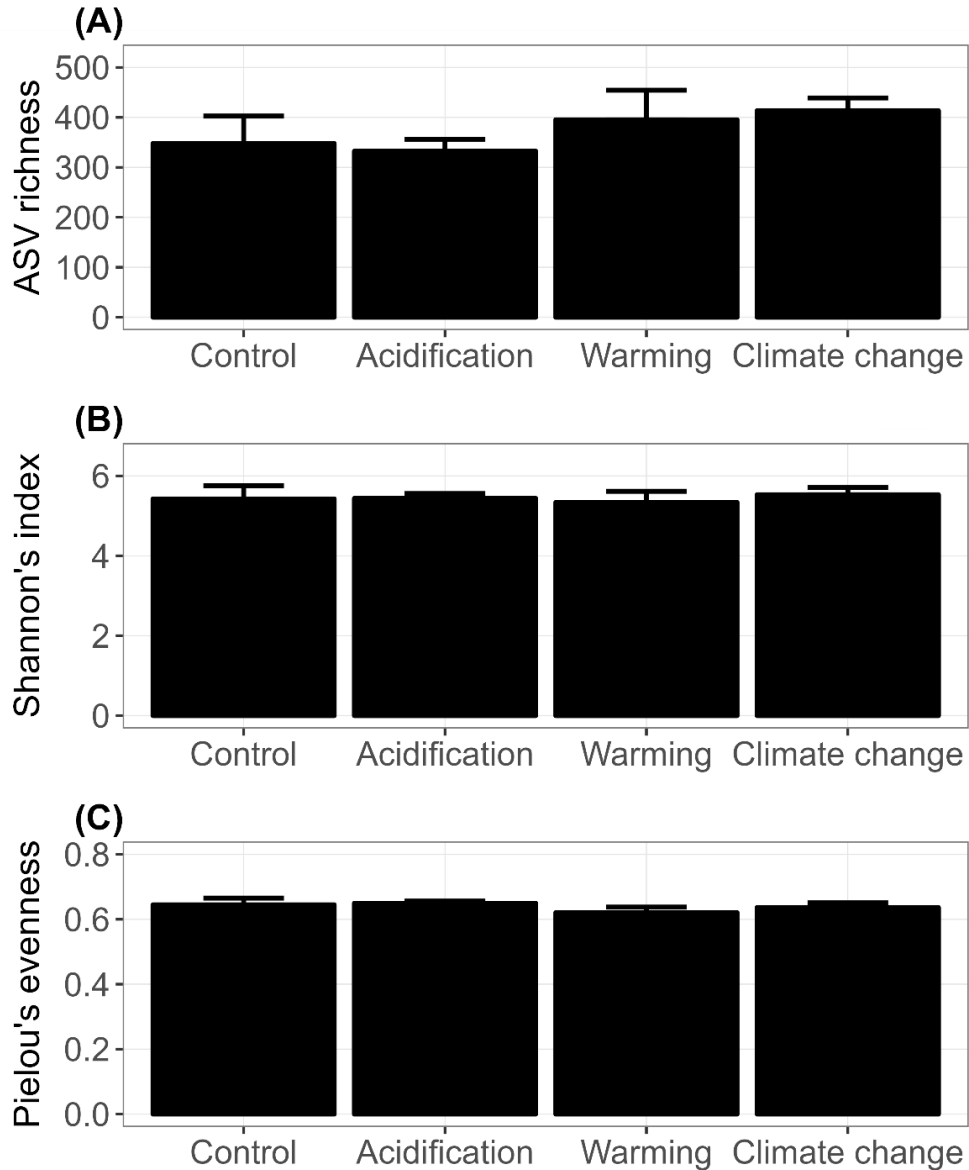
745 Wahl, M., Jensen, P.R., Fenical, W., 1994. Chemical control of bacterial epibiosis on ascidians.
746 *Marine Ecology Progress Series* 110, 45–57.

747 Wang, Z., Tsementzi, D., Williams, T.C., Juarez, D.L., Blinebry, S.K., Garcia, N.S., Sienkiewicz,
748 B.K., Konstantinidis, K.T., Johnson, Z.I., Hunt, D.E., 2021. Environmental stability
749 impacts the differential sensitivity of marine microbiomes to increases in temperature and
750 acidity. *The ISME Journal* 15, 19–28. <https://doi.org/10.1038/s41396-020-00748-2>

751 Wannicke, N., Frey, C., Law, C.S., Voss, M., 2018. The response of the marine nitrogen cycle to
752 ocean acidification. *Global Change Biology* 24, 5031–5043.
753 <https://doi.org/10.1111/gcb.14424>

754 Welsh, D.T., Castadelli, G., 2004. Bacterial nitrification activity directly associated with isolated
755 benthic marine animals. *Marine Biology* 144, 1029–1037. <https://doi.org/10.1007/s00227->
756 003-1252-z
757 Wind Europe, 2021. Wind energy in Europe: 2020 Statistics and the outlook for 2021-2025.
758 Wu, L., An, Z., Zhou, J., Chen, F., Liu, B., Qi, L., Yin, G., Dong, H., Liu, M., Hou, L., Zheng,
759 Y., 2022. Effects of aquatic acidification on microbially mediated nitrogen removal in
760 estuarine and coastal environments. *Environ. Sci. Technol.* 56, 5939–5949.
761 <https://doi.org/10.1021/acs.est.2c00692>
762
763

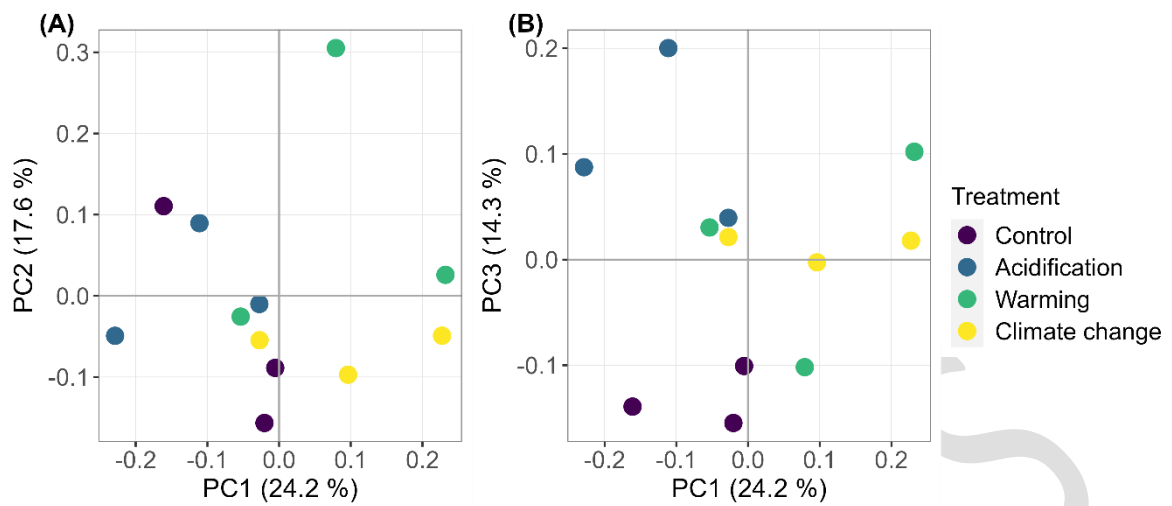
Accepted MS



764
 765
 766 **Figure 1** Influence of experimental treatments (“Treatment” factor, four levels: “Control”, “Acidification,”
 767 Warming” and “Climate change”) on (A) species richness (amplicon sequence variants ASV), (B) Shannon-
 768 Wiener’s index and (C) Pielou’s evenness for microbial communities sampled on the shell of mussels after
 769 six weeks of incubation. Results are given as mean + SE. $N = 3$ per experimental treatment.

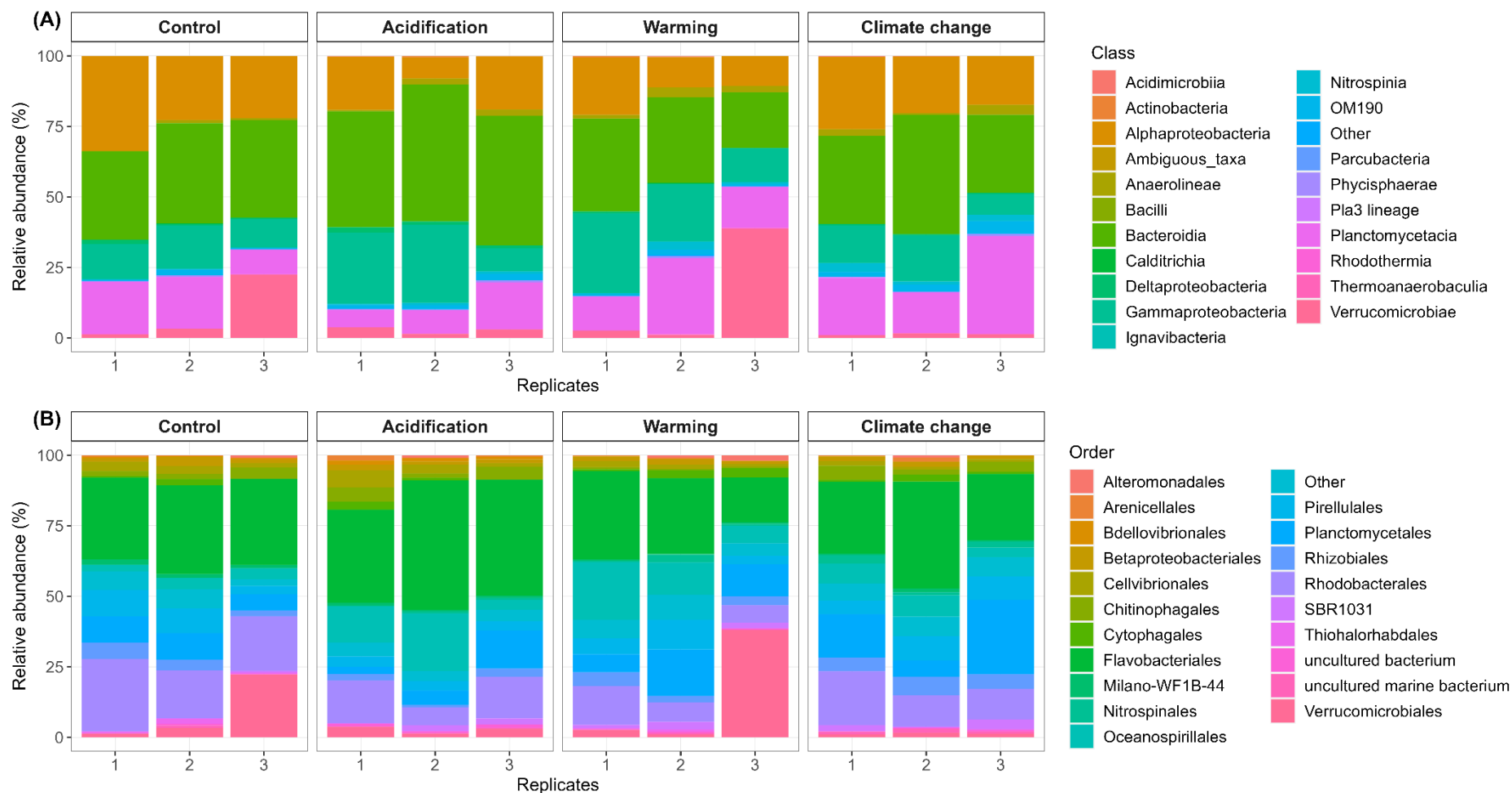
770
 771

772



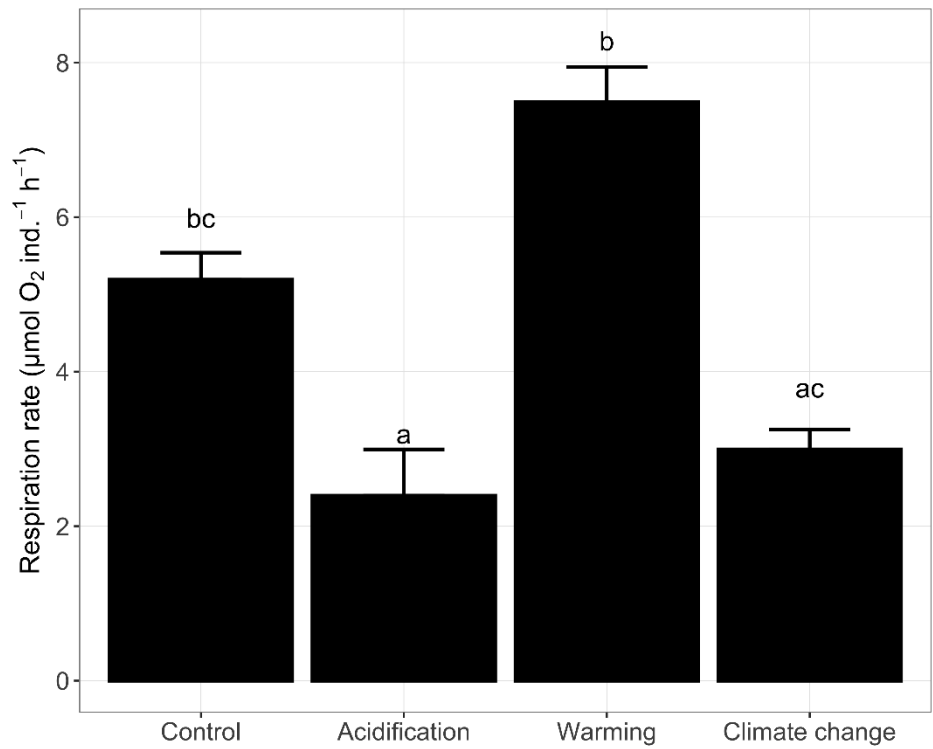
773

774 **Figure 2** Principal coordinate analysis (PCoA) ordination based on GUniFrac distance matrix evaluating
775 the influence of simulated seawater acidification and/or warming on microbial communities sampled on
776 the shell of mussels after six weeks of incubation. $N = 3$ per experimental treatment.

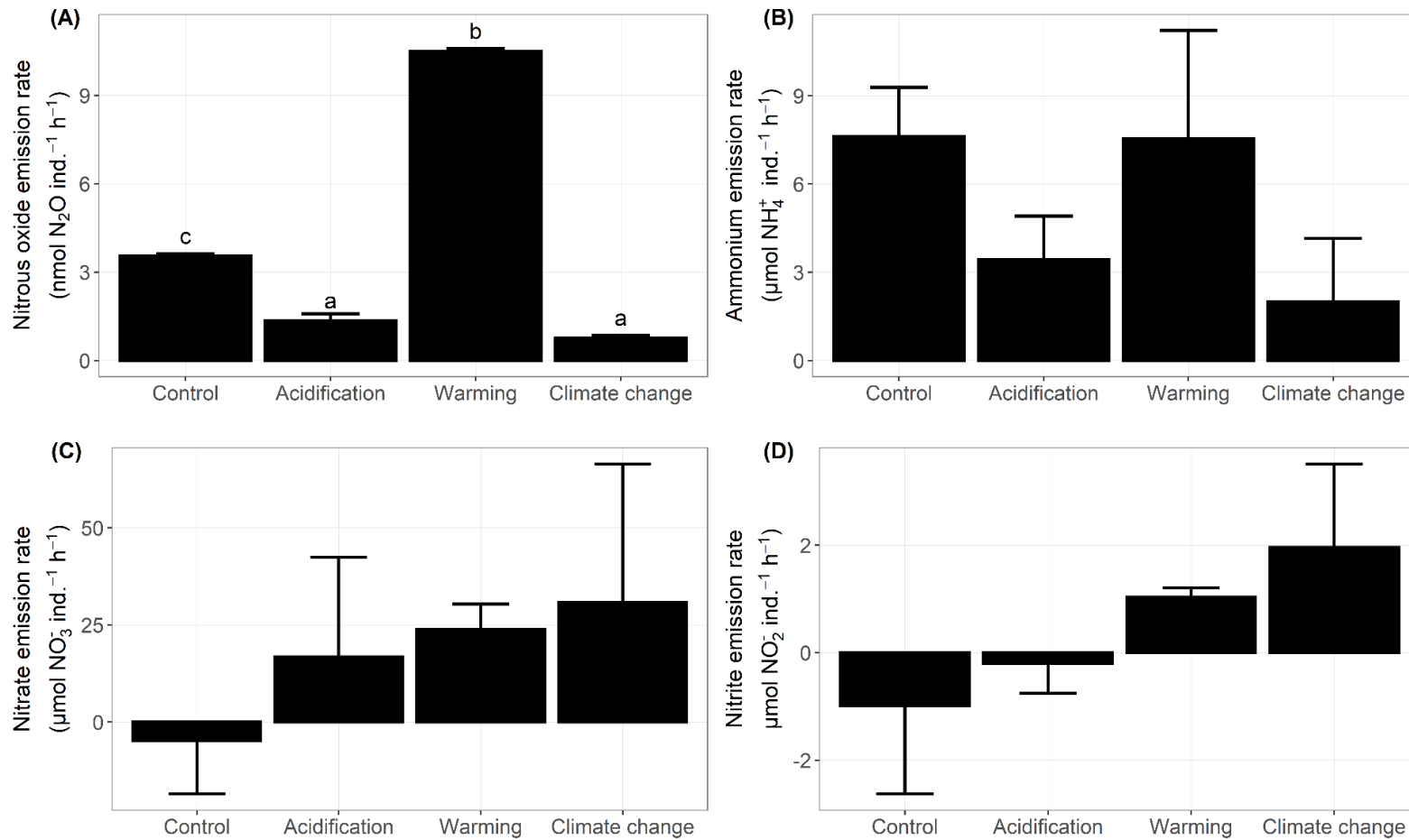


777

778 **Figure 3** Influence of experimental treatments (“Control”, “Acidification”, “Warming” and “Climate change”) on the relative abundance of the dominant
 779 amplicon sequence variants (ASV) at the class (A) and order (B) levels on the shell of mussels *Mytilus edulis* after six weeks of incubation. The twenty most
 780 abundant microbial classes and orders are shown. $N = 3$ per experimental treatment.



781
 782 **Figure 4** Influence of experimental treatments (“Control”, “Acidification”, “Warming” and “Climate
 783 change”) on the mean aerobic respiration rates (+ SE) of microbial biofilm developing on the shell
 784 surface of blue mussels *Mytilus edulis* after six weeks of incubation. Results of Tukey posthoc tests on
 785 the significant effects of experimental treatment are shown (different groups of letters indicate
 786 significant differences, $p < 0.05$). Results are given as mean + SE. $N = 3$ per experimental treatment.

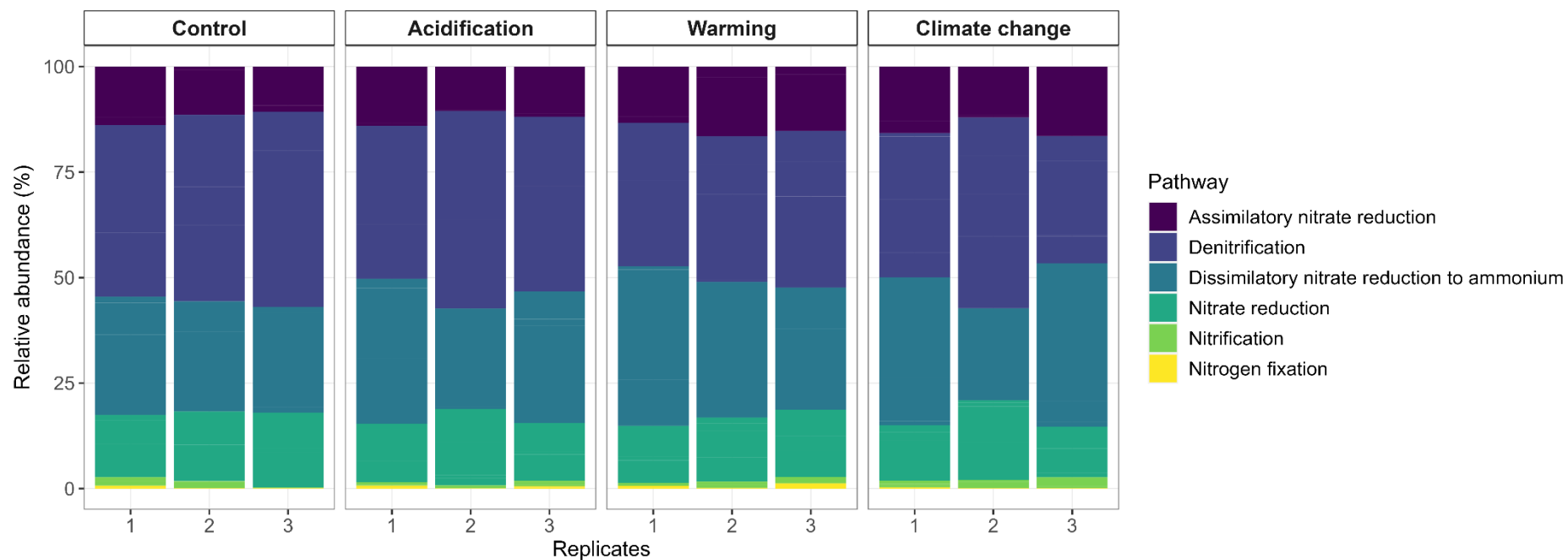


787

788 **Figure 5** Influence of experimental treatments (“Control”, “Acidification”, “Warming” and “Climate change”) on the mean production or consumption rates of

789 (A) nitrous oxide N₂O, (B) ammonium NH₄⁺; (C) nitrate NO₃⁻ and (D) nitrite NO₂⁻. Results of Tukey posthoc tests on the significant effects of experimental

790 treatment are shown (different groups of letters indicate significant differences, *p* < 0.05). Results are given as mean + SE. *N* = 3 per experimental treatment.



791

792 **Figure 6** Influence of experimental treatments (“Control”, “Acidification”, “Warming” and “Climate change”) on the relative abundance (%) of predicted nitrogen
 793 transformation pathways (PICRUST analysis) associated to the microbiome on the shell of mussels *Mytilus edulis* after six weeks of incubation. Pathways are of
 794 the sum of counts of KEGG ortholog genes. $N = 3$ per experimental treatment.

795 **Table 1** Relative abundance (mean \pm SE, %) of the most abundant taxa (class and order levels) in microbial communities on the shell of blue mussels *Mytilus*
 796 *edulis* after a six-week incubation period under different experimental treatments (“Control”, “Acidification”, “Warming” and “Climate change”).

CLASS	Control	Acidification	Warming	Climate change
Alphaproteobacteria	25.9 \pm 3.9	15.1 \pm 3.7	13.9 \pm 3.3	21.0 \pm 2.4
Bacteroidia	34.1 \pm 1.4	45.1 \pm 2.2	27.6 \pm 4.2	33.8 \pm 4.3
Gammaproteobacteria	12.5 \pm 1.4	20.3 \pm 6.2	20.0 \pm 4.5	12.2 \pm 2.6
Planctomycetacia	15.1 \pm 3.2	10.5 \pm 3.1	17.7 \pm 4.5	23.0 \pm 5.9
<i>Total proportion of the total community</i>	87.5 \pm 6.3	90.9 \pm 0.6	79.2 \pm 11.4	90.1 \pm 1.8
ORDER				
Alteromonadales				
Cellvibrionales				
Flavobacteriales	30.5 \pm 0.9	39.9 \pm 3.8	24.7 \pm 4.7	29.1 \pm 4.4
Oceanospirillales	3.4 \pm 0.5	12.1 \pm 4.9	12.6 \pm 4.0	5.9 \pm 1.3
Pirellulales	7.0 \pm 2.0	3.5 \pm 0.2	6.3 \pm 2.1	7.5 \pm 1.3
Planctomycetales	8.0 \pm 1.2	7.0 \pm 3.2	11.3 \pm 2.9	15.5 \pm 5.9
Rhizobiales	3.8 \pm 1.1	2.1 \pm 0.6	3.5 \pm 0.9	5.5 \pm 0.5
Rhodobacterales	20.5 \pm 2.7	12.1 \pm 2.8	8.9 \pm 2.4	13.8 \pm 2.5
Verrucomicrobiales	9.0 \pm 6.7	2.7 \pm 0.7	14.0 \pm 12.1	1.4 \pm 0.1
<i>Total proportion of the total community</i>	82.2 \pm 2.5	79.3 \pm 3.1	81.3 \pm 3.2	78.7 \pm 0.4

797

798

799
800

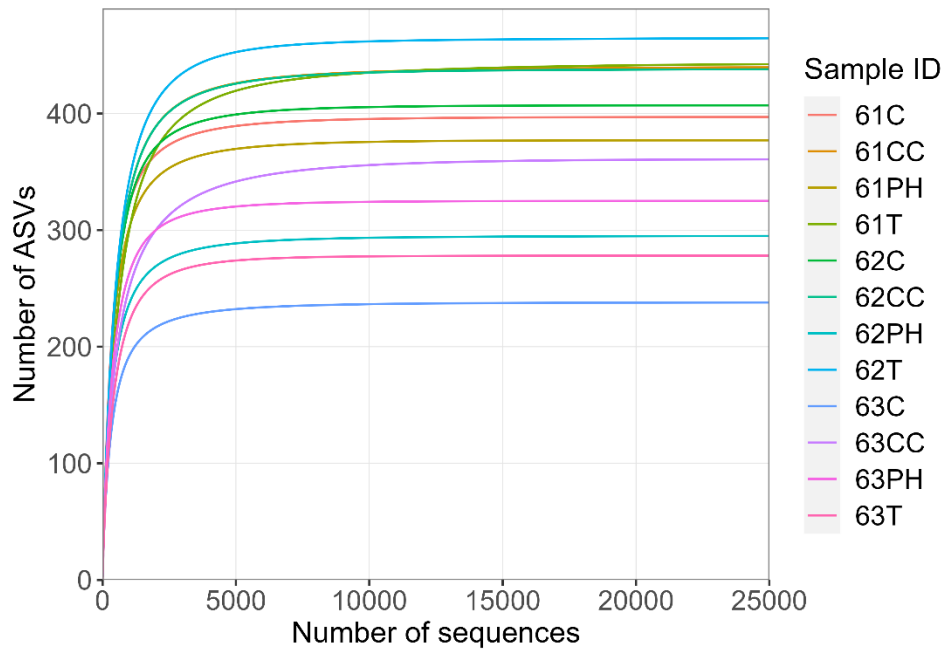
Supplementary data

801 **Supplement S1** Summary of the physico-chemical parameters of the mesocosm waters for the four
802 experimental treatments. Values are given as mean \pm standard deviation. pH was measured on the NBS
803 scale.

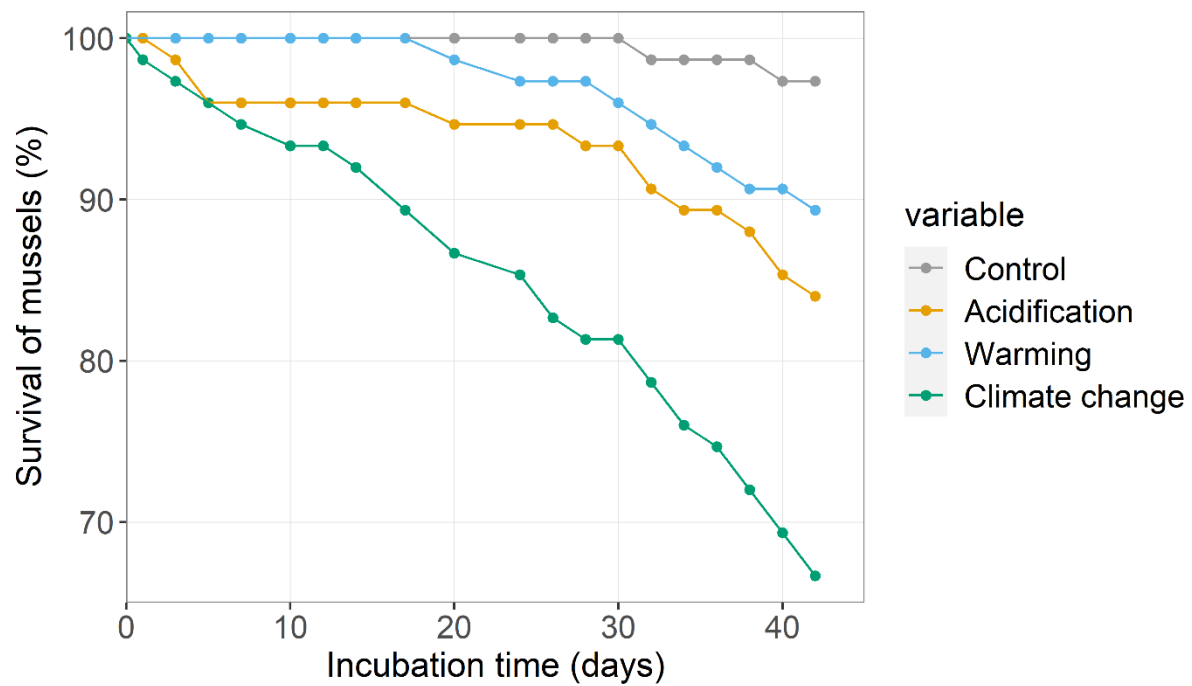
	Temperature (°C)	pH	Salinity	Total alkalinity ($\mu\text{mol kg}^{-1}$)	pCO ₂ (μatm)	Dissolved inorganic carbon C _T $\mu\text{mol kg}^{-1}$	Bicarbonate ion HCO ₃ ⁻ ($\mu\text{mol kg}^{-1}$)
Control	20.0 \pm 0.1	8.0 \pm 0.0	33.0 \pm 0.5	2106.9 \pm 247.5	453.3 \pm 45.7	1910.6 \pm 225.6	1753.9 \pm 225.6
Acidification	20.0 \pm 0.3	7.6 \pm 0.0	32.4 \pm 0.4	1984.8 \pm 280.1	966.6 \pm 127.1	1809.0 \pm 270.8	70.0 \pm 25.0
Warming	23.2 \pm 0.2	8.0 \pm 0.0	33.8 \pm 0.5	2113.3 \pm 268.5	441.9 \pm 39.8	1711.4 \pm 237.3	161.7 \pm 25.0
Climate change	23.1 \pm 0.3	7.7 \pm 0.0	33.0 \pm 0.5	2037.7 \pm 317.3	990.2 \pm 145.9	1834.8 \pm 306.0	81.4 \pm 28.0

804

Accepted MS



Supplement S2 Rarefaction curves of microbiomes on the shell surface of blue mussels *Mytilus edulis* after six weeks of incubation. All samples are plotted.



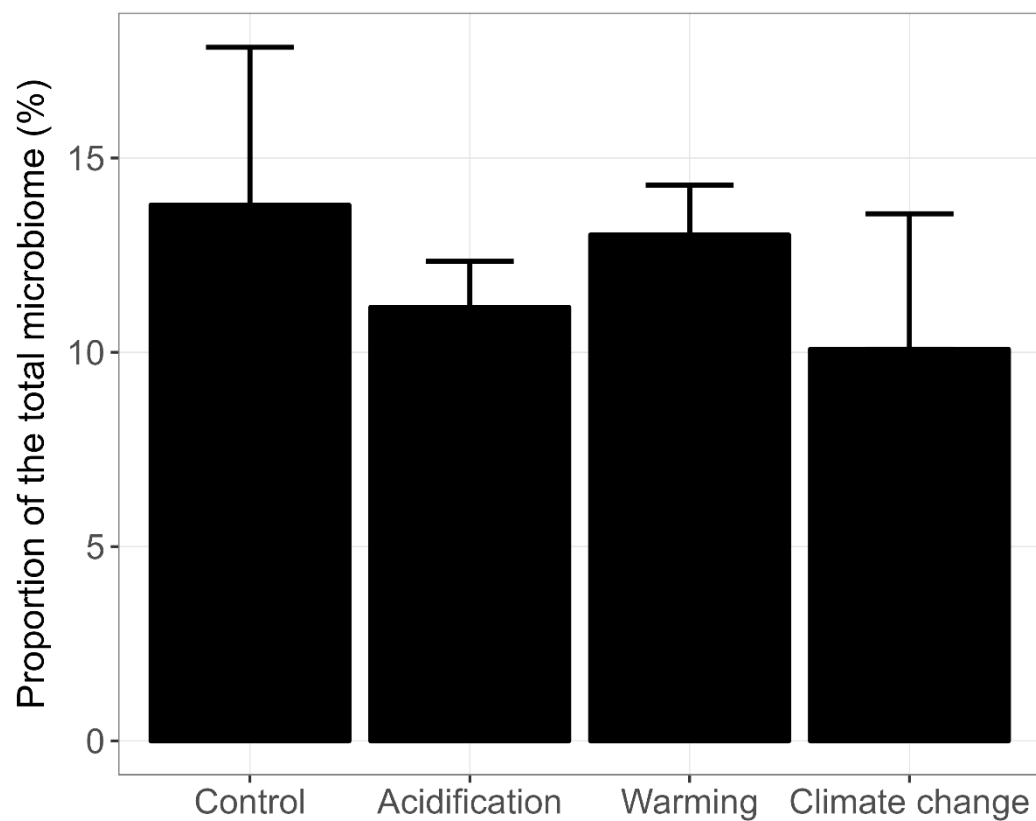
Supplement S3 Survival of blue mussels *Mytilus edulis* over six weeks (42 days) of incubation under four experimental treatments. $N = 75$ individuals per experimental treatment.

Accepted

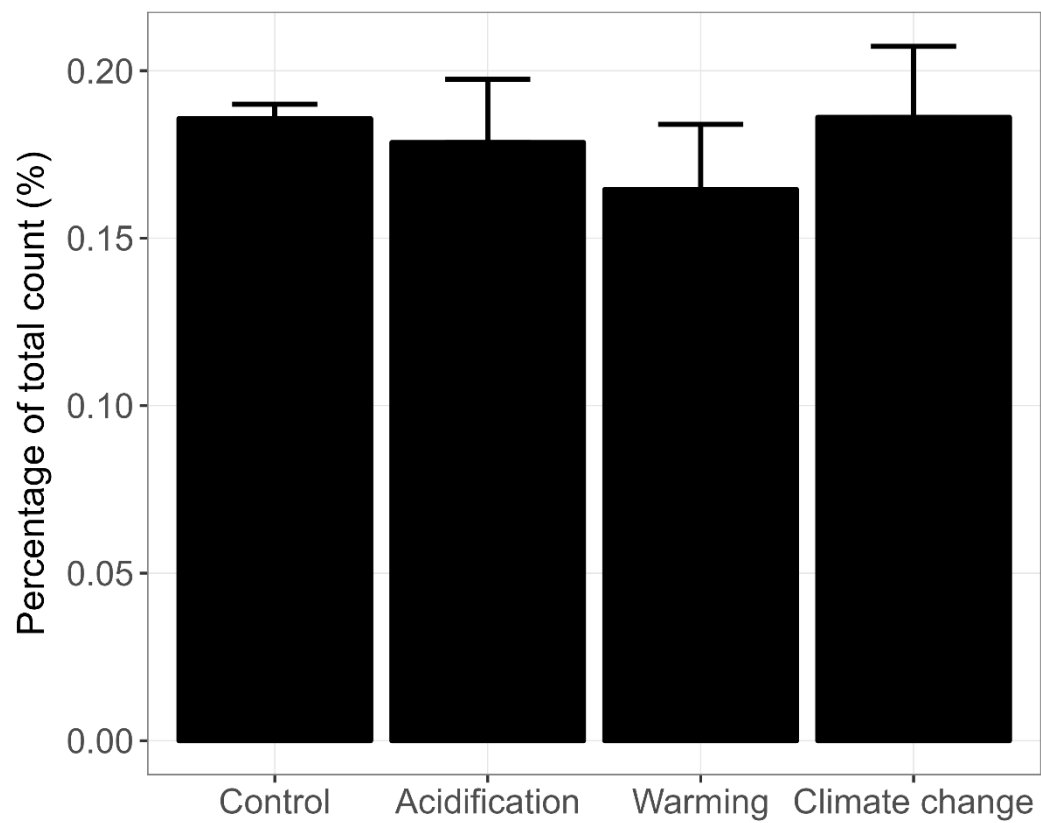
Supplement S4 Results of sequence data processing for the different groups of samples according to the experimental treatments.

Experimental treatment	Number of replicates	Number of sequences before the filtering steps (min-max)	Number of sequences after the filtering steps (min-max)	Number of ASV (min-max)
Control	3	36,322-51,163	36,011-50,689	226-386
Acidification	3	44,828-49,524	44,259-48,838	270-351
Warming	3	32,857-67,837	32,170-67,180	261-438
Climate change	3	58,340-64,835	57,830-64,366	332-417

Accepted MS



Supplement S5 Percentage of the total bacterial community belonging to the core microbiome for biofilms on the shell of blue mussels *Mytilus edulis* after six weeks of incubation under different experimental treatments. Core microbiomes were identified as a list of amplicon sequence variants (ASV) shared between 90 % of the mussel biofilm samples. $N = 15$ shared ASVs for mussel biofilm samples.



Supplement S6 Percentage of the KEGG ortholog genes involved in the nitrogen metabolism in the microbial biofilms on the shell of blue mussels *Mytilus edulis* after six weeks of incubation under different experimental treatments.

1
2

3
4
5
6
7
8
9
10
11
12
13
14
15
16

Accepted MS